Neutrino Interactions in the MINOS Near Detector

D.Naples
University of Pittsburgh

(for the MINOS Collaboration)

DPF 2006
Honolulu, HI
Oct 29-Nov 3, 2006

Outline

- MINOS Overview
  - NuMI Beam
  - Minos Near Detector
- Low Energy Neutino Cross Section
- CC Cross Section Analysis
- Flux Measurement Technique
  - Flux Results
- $\overline{\nu}$ Data Sample
- Structure Functions in MINOS
- Conclusions

MINOS Overview

- Main goal of MINOS: measure oscillation parameters in 2→3 sector.
- Purpose of Near Detector:
  - Measure unoscillated beam spectrum.
  - Understand cross section and detector modeling.
- Near Det. has large event samples.

  → *Can be used to study neutrino (and antineutrino) interactions and cross sections.*

Two detectors: *near* detector at Fermilab (L∼1km), *far* detector at Soudan MN (L∼735km)

- Focus of talk: cross section measurements using MINOS near detector sample.

Fermilab's NuMI Beam

- Movable target, allows three beam configurations, LE, ME, and HE.
- **Majority of data ($\sim$ 95%) taken in low energy configuration (LE-10).**
  - LE-10 Event Composition: 92.9%ν_μ 5.8% $\overline{\nu_\mu}$, 1.3% ($\nu_e + \overline{\nu_e}$)

Near Detector CC events (thru Oct. 2006).

Beam	Target z (cm)	CC Sample
LE-10	**-10**	$\mathbf{2.1 \times 10^6}$ (ν)
LE-10	**-10**	$\mathbf{1.7 \times 10^5}$ ($\overline{\nu}$)
ME	-100	1.9×10^4
HE	-250	3.7×10^4

Total Exposure of 1.7E20 PoT

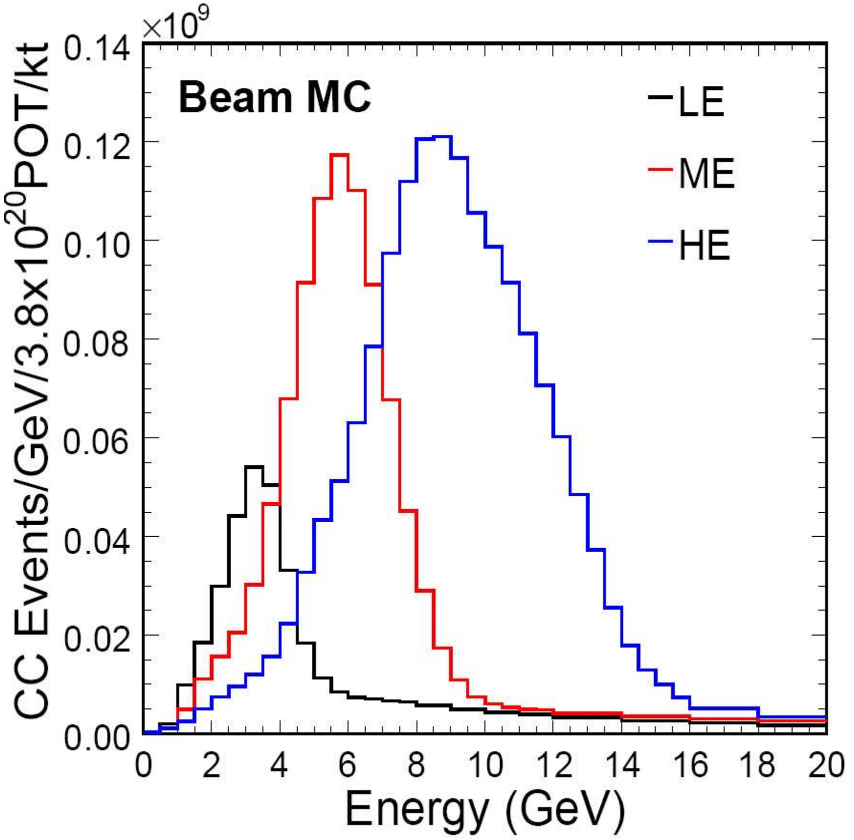

- MINOS LE-10 near detector data $\rightarrow$ *largest data sample for neutrino interactions in this energy range to date.*

MINOS Near Detector

Magnetized tracking calormeter

- 1cm thick planes of scintillator (4.1cm wide strips).
- Sampling every 2.54cm steel.
  - Coarser sampling in downstream spectrometer region (every 5 planes of steel)
- Magnetized steel plates $\langle B \rangle = 1.2\text{T}$

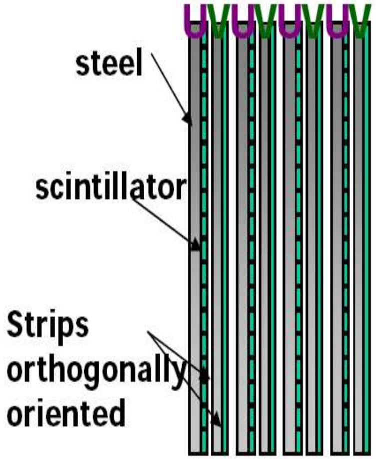

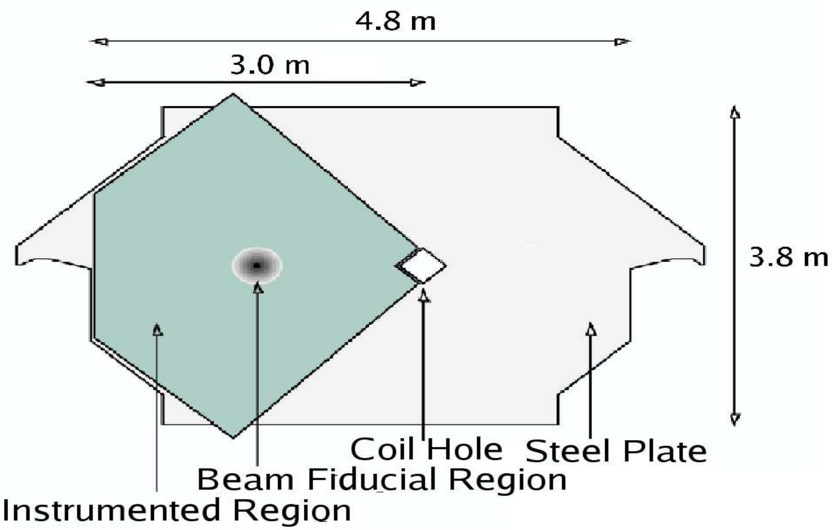

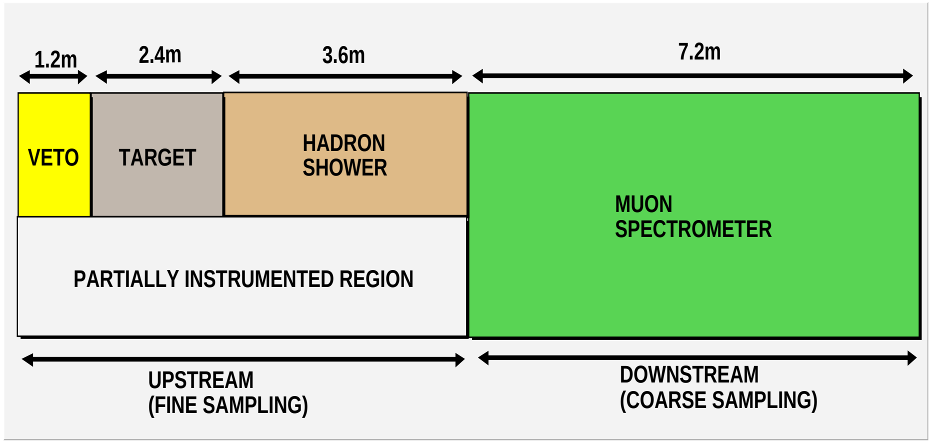

Contributions to Neutrino Scattering

- $\sigma_{\mathrm{TOT}} = \sigma_{\mathrm{QE}} + \sigma_{\mathrm{RES}} + \sigma_{\mathrm{DIS}}$
- Quasi Elastic (QE)
  $\nu n \longrightarrow \mu^- p, \overline{\nu} p \longrightarrow \mu^+ n$
  $\nu(\overline{\nu})$ scatters off an entire nucleon.
- Resonance $\nu N \longrightarrow \nu N^*$
  $\nu_\mu p(n) \longrightarrow \mu^- \pi^+ p(n)$
  $\nu_\mu n \longrightarrow \mu^- \pi^0 p$
  Excited nucleon decays into low multiplicity final states.
- Deep Inelastic Scattering (DIS)
  $\nu(\overline{\nu}) N \longrightarrow \mu^-(\mu^+) X$
  $\nu(\overline{\nu})$ scatters off nucleon constituents.
- **These contributions are not precisely known at low energies.**

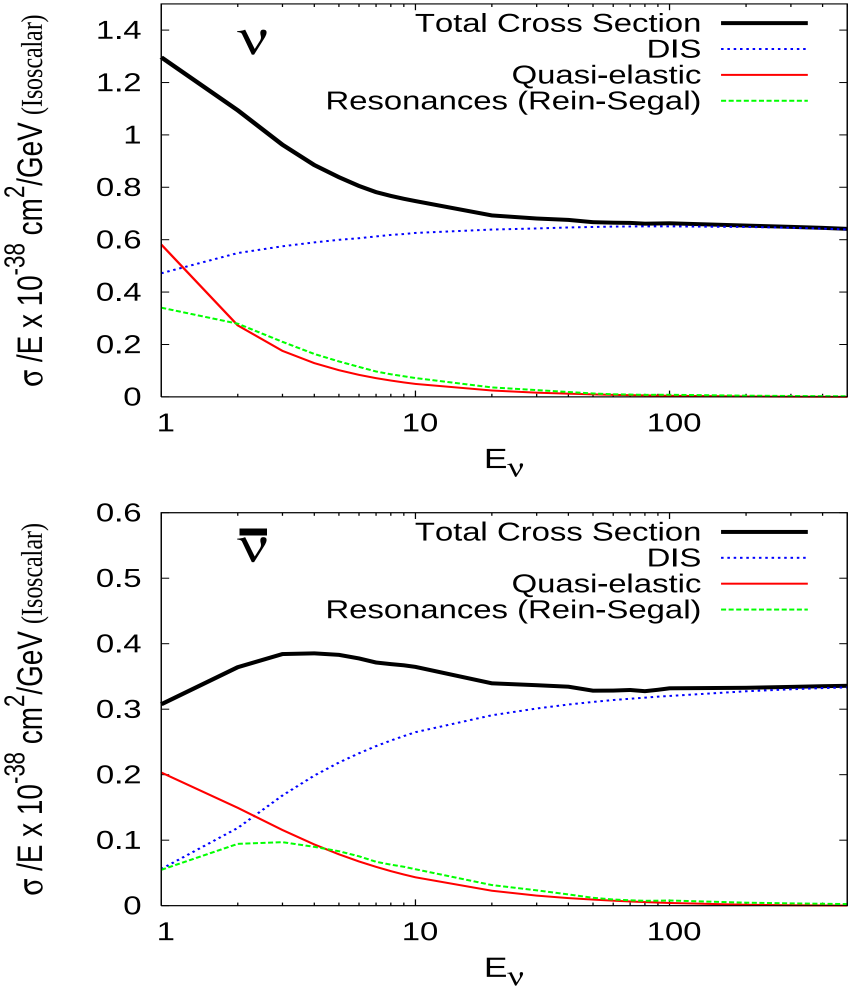

Total cross section features:

- $\frac{\sigma}{E}$ rises at low energy due to contributios from QE and Resonance processes. (both saturate a low energy- few GeV region).
- At high energy $\frac{\sigma}{E}$ is roughly flat and dominated by DIS.

CC Cross Sections in MINOS

- MINOS coarse-grained detector is not ideal for identifying individual final state particles $\longrightarrow$ except for μ.
  - Look at inclusive CC cross section and DIS cross section.

- Energy dependence of total CC cross section (range $\sim$5-50 GeV).

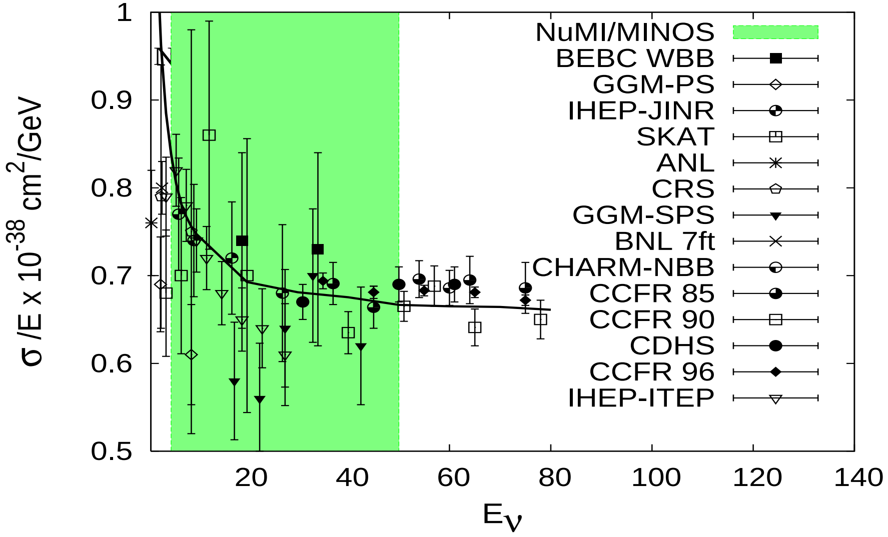

- $\star$ Existing data is of limited precision $\stackrel{\sim}{>}$10%
- $\star$ MINOS range covers interesting low energy region where all three process contribute.

- DIS Cross Section and Structure Functions

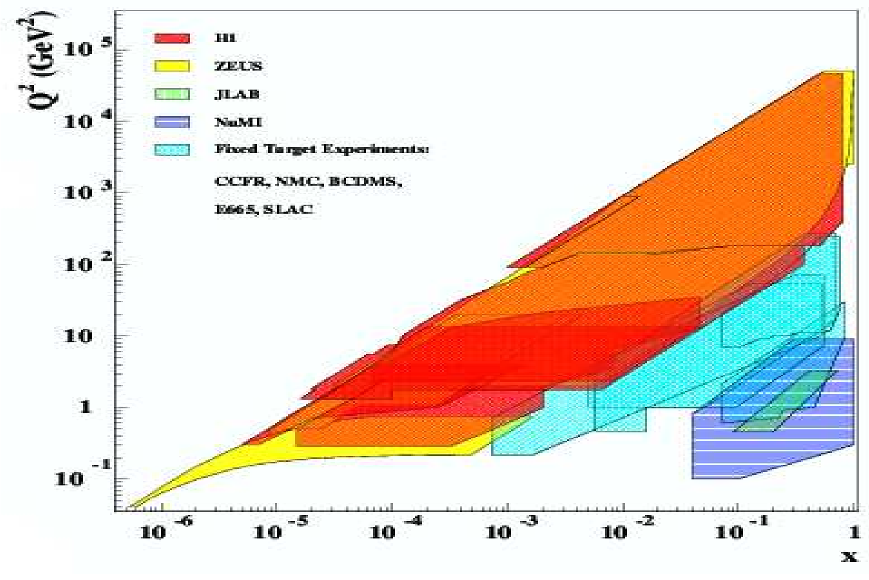

- $\star$ New kinematic regime for ν N SFs
- $\star$ High-x low Q^2 : Good coverage in charged-lepton scattering, but little neutrino data.

Charged-Current Neutrino Scattering

- DIS is the largest contribution to the MINOS event sample.

DIS 62%, RES 21%, QE 17%

  - For $E_\nu > 5$ GeV, DIS is the dominant process.

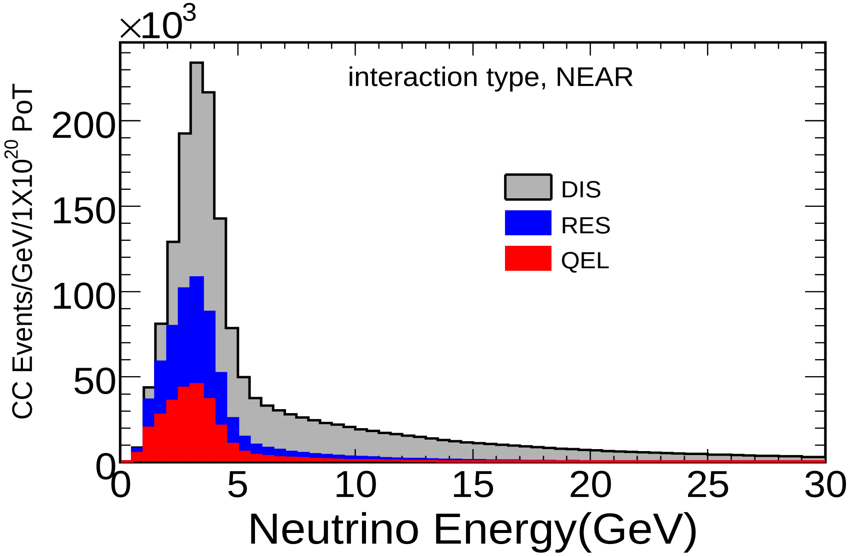

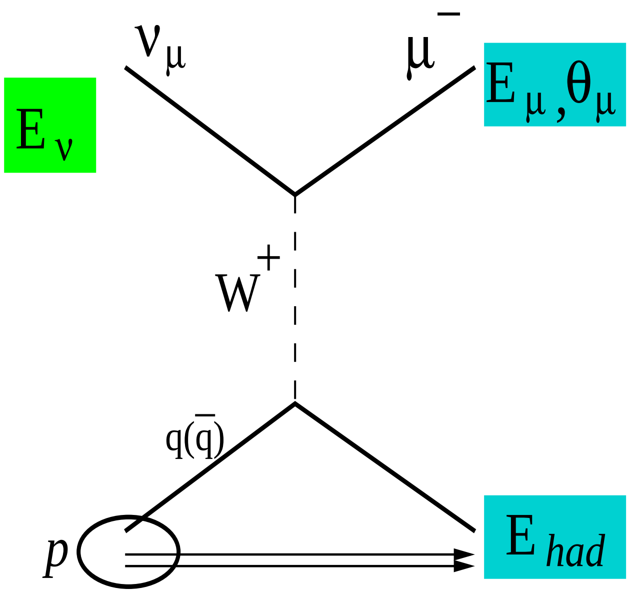

Reconstruct $E_\nu = E_{HAD} + E_\mu$

Shower energy resolution: 55%/$\sqrt{E}$

Muon Momentum resolution: 6% range,13% curvature

$Q^2 = 4E_\nu E_\mu \sin^2 \frac{\theta}{2}$,	Squared four momentum transfer
$x = \frac{Q^2}{2ME_{HAD}}$,	Fractional quark momentum
$y = \frac{E_{HAD}}{E_\nu}$,	Inelasticity
$W^2 = M^2 + 2ME_{HAD} - Q^2$,	Squared fi nal state invariant mass

CC Event Selection

- 1 good fit track
- Vertex contained inside fiducial volume.
  - Upstream 'target' region.
  - Centered on beam spot.
  - Fiducial mass ~4ton.
- Select sign of the muon, μ^- for ν_μ, μ^+ for $\overline{\nu_\mu}$,
- CC event selection kinematic cut: $E_\mu > 2$GeV
  - Stopping, momentum from range
  - Exiting, momentum from curvature
  - Removes NC contamination.
- Reconstructed neutrino energy $E_\nu > 5$ GeV.

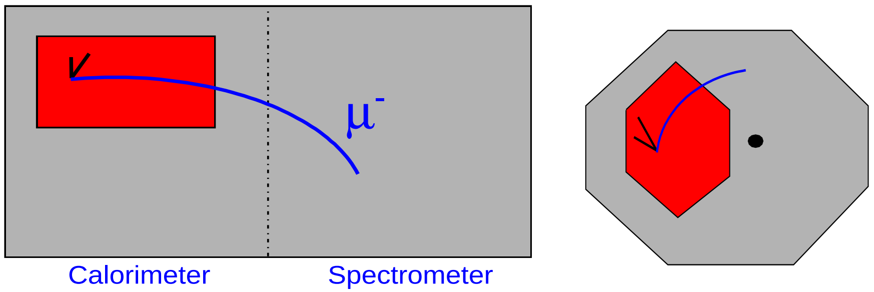

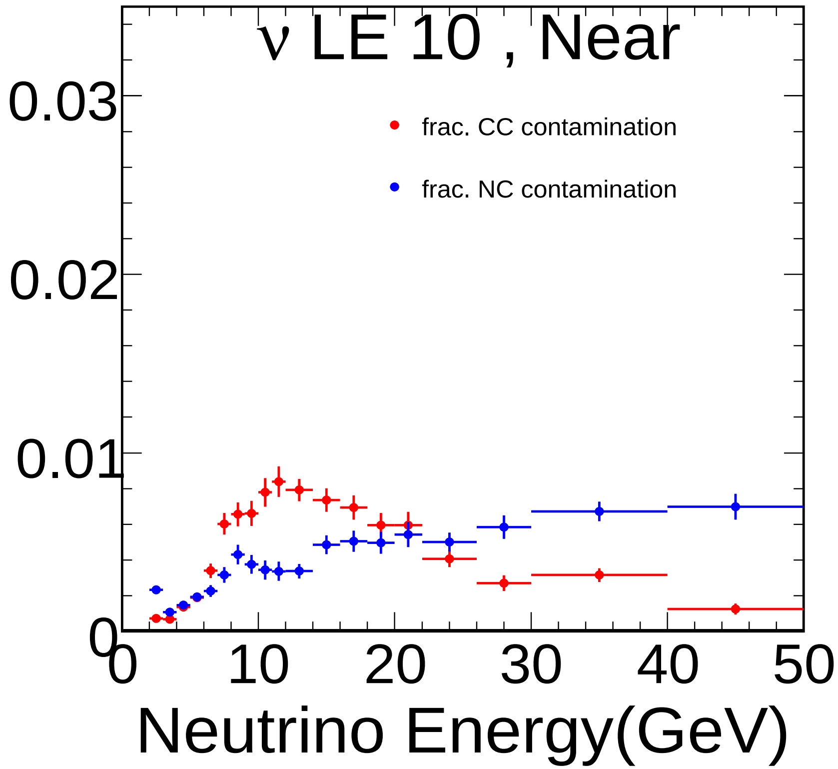

Cross Section Extraction

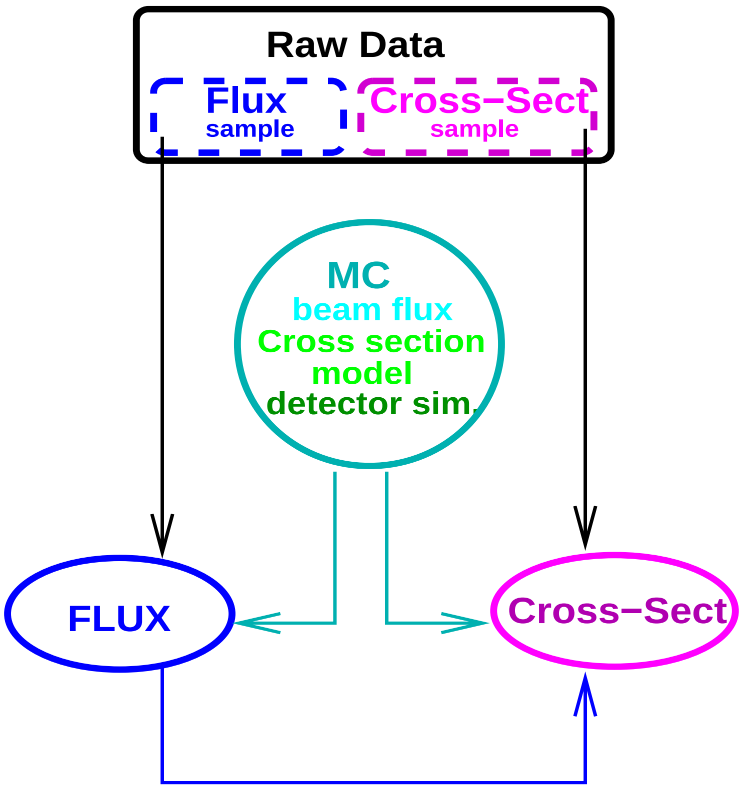

- Two samples: Flux, Cross section
- Monte Carlo used to apply corrections for acceptance and smearing.

  Ingredients

  - Input beam flux (GEANT3 based beamline simulation, production model FLUKA05).
  - Cross section model (NEUGEN3): uses Bodek-Yang duality model,(BY-GRV98LO), tuned to data in DIS/res. overlap region.
  - Detector simulation.
- Determine Flux from 'flux' sample (next slide).
- Extract cross section, $\frac{d^2\sigma}{dxdy}^{\nu(\overline{\nu})} = \frac{1}{\Phi(E)} \frac{d^2N}{dxdy}^{\nu(\overline{\nu})}$.

Cross Section Extraction

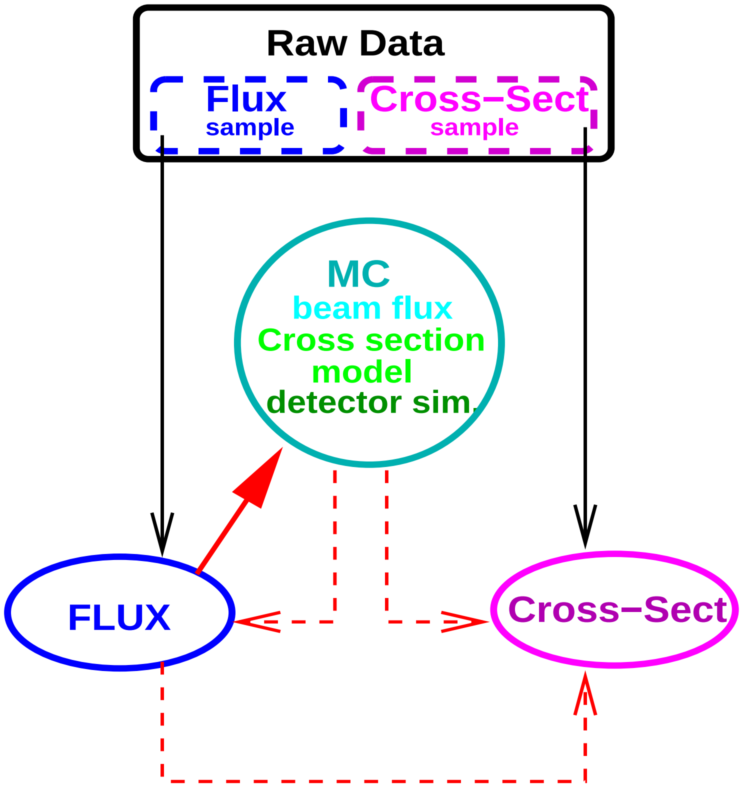

- Two samples: Flux, Cross section
- Monte Carlo used to apply corrections for acceptance and smearing.

  Ingredients

  - Input beam flux (GEANT3 based beamline simulation, production model FLUKA05).
  - Cross section model (NEUGEN3): uses Bodek-Yang duality model,(BY-GRV98LO), tuned to data in DIS/res. overlap region.
  - Detector simulation.
- Determine Flux from 'flux' sample (next slide).
- Extract cross section, $\frac{d^2\sigma}{dxdy}^{\nu(\overline{\nu})} = \frac{1}{\Phi(E)} \frac{d^2N}{dxdy}^{\nu(\overline{\nu})}$.
- Iterate with new (measured) flux

Cross Section Extraction

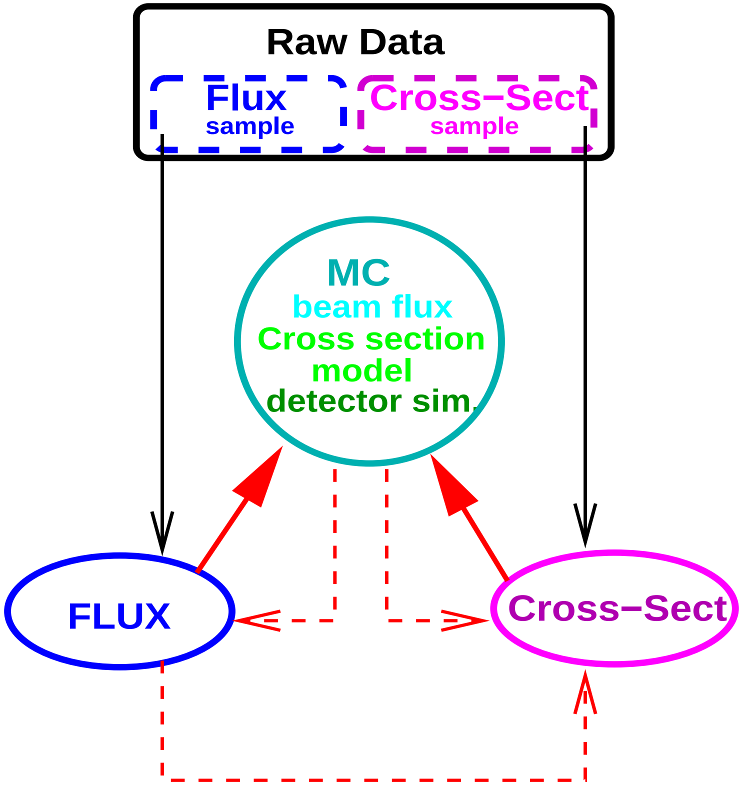

- Two samples: Flux, Cross section
- Monte Carlo used to apply corrections for acceptance and smearing.

  Ingredients

  - Input beam flux (GEANT3 based beamline simulation, production model FLUKA05).
  - Cross section model (NEUGEN3): uses Bodek-Yang duality model,(BY-GRV98LO), tuned to data in DIS/res. overlap region.
  - Detector simulation.
- Determine Flux from 'flux' sample (next slide).
- Extract cross section, $\frac{d^2\sigma}{dxdy}^{\nu(\overline{\nu})} = \frac{1}{\Phi(E)} \frac{d^2N}{dxdy}^{\nu(\overline{\nu})}$.
- Iterate with new (measured) flux
- Fit differential cross section and input as new cross section model... iterate.

Relative Flux Extraction Method

- ▶ Use inclusive low $\nu(=E_{\mathrm{HAD}})$ cross section to get flux shape.
  - *Similar method used at higher energy (CCFR/NuTeV)→ adapt to lower energies.*

$$\frac{d^2\sigma^{\nu,\overline{\nu}}}{dxd\nu} = \frac{G^2M}{\pi}\left[\left(1-\frac{\nu}{E}-\frac{Mx\nu}{2E^2}+\frac{\nu^2}{2E^2}\frac{1+2Mx/\nu}{1+R}\right)F_2(x) \pm \frac{\nu}{E}\left(1-\frac{\nu}{2E}\right)xF_3(x)\right]$$

Integrate $d^2\sigma/dxd\nu$ over x for fixed ν:

$$\frac{d\sigma}{d\nu} = A\left(1+\frac{B}{A}\frac{\nu}{E}-\frac{C}{A}\frac{\nu^2}{2E^2}\right)$$

$$A = \frac{G^2M}{\pi}\int F_2(x)dx$$

$$B = -\frac{G^2M}{\pi}\int \left(F_2(x) \mp xF_3(x)\right)dx$$

$$C = B - \frac{G^2M}{\pi}\int F_2(x)\left(\frac{1+\frac{2Mx}{\nu}}{1+R(x)}-\frac{Mx}{\nu}-1\right)dx$$

- ▶ At low ν and high E_ν
  $\Rightarrow$ $(\frac{\nu}{E})$ and $(\frac{\nu}{E})^2$ terms are small.

$$\frac{d\sigma}{d\nu}^{\nu}_{\lim \nu\to 0} = \frac{d\sigma}{d\nu}^{\overline{\nu}}_{\lim \nu\to 0} = A$$ *constant, independent of* E_ν. $\to \Phi(E) \propto N(E, \nu < \nu_o)$.

- ▶ For MINOS require $\nu < 1$GeV and extract flux for $E_\nu > 5$ GeV.

1. Count events at low ν, $N(E, \nu < 1\mathrm{GeV})$
2. Use cross section model to correct for energy dependence in low-ν sample, $c(E) = \frac{\sigma_{asym}(\nu<1))}{\sigma(\nu<1)}$
3. $\Phi(E) \propto c(E)N(E, \nu < 1\mathrm{GeV})$

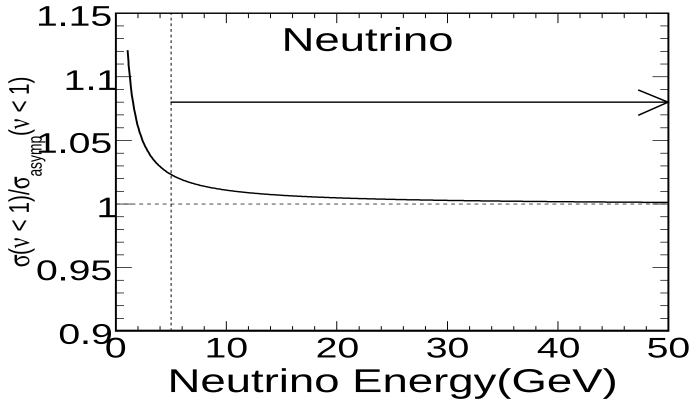

Near Detector Extracted Flux

LE-10 Data Sample 1.0E20 PoT (June-Dec 2005).

- ▶ Flux sample: CC events with $\nu < 1$ GeV, ($E_\nu > 5$ GeV)
  - Data corrected for acceptance and smearing using MC model.

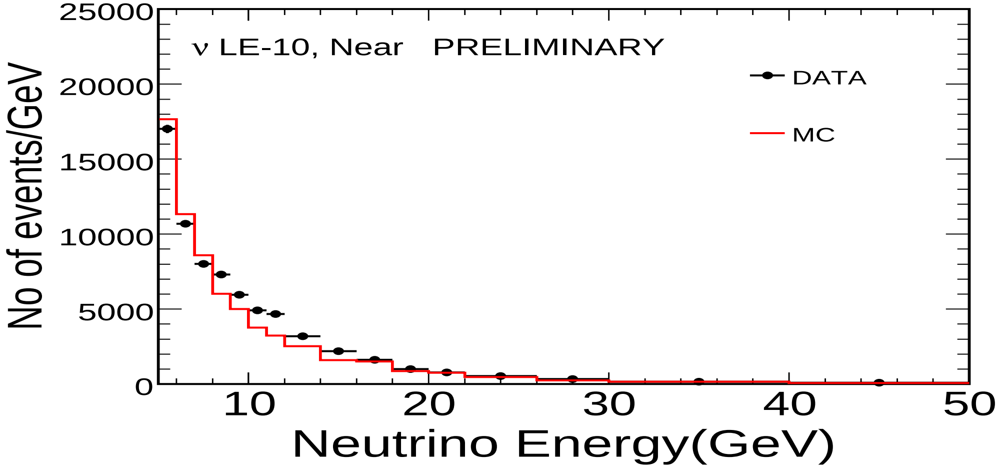

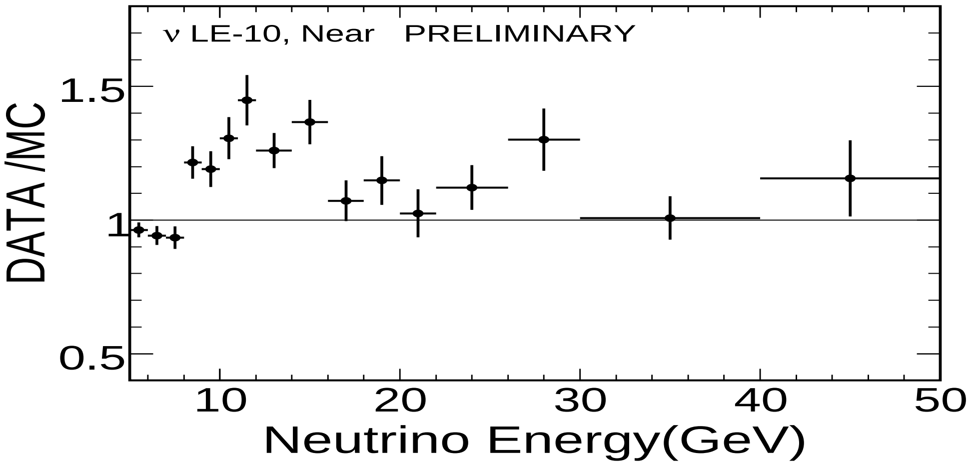

- ▶ Extracted data flux for 1E20 PoT (unnormalized).
  - Compare with MC which uses default beam flux model (GEANT3 + FLUKA05 production).
    - ⋆ MC normalized to 1.0E20 PoT.
- ▶ Shows large discrepancy (up to 40% $\pm$ 10%) in the $E_\nu > 10\mathrm{GeV}$ GeV region (outside the beam focusing peak).
  - Beam model flux uncertainties are large (∼15%) and dominated by production uncertainties in this region.

Reconstructed Energy Spectrum

- Total cross section sample:
  - All CC events (events with well reconstructed muon, $E_\mu > 2\mathrm{GeV}$).
- Effect of flux re-iteration on reconstructed CC energy spectrum.
  - Nominal MC (blue curve) using GEANT3+FLUKA05 beam flux.
  - MC reweighted by low-ν extracted flux (red curve).
  - Data/MC agreement improves dramatically after one reiteration of the flux.

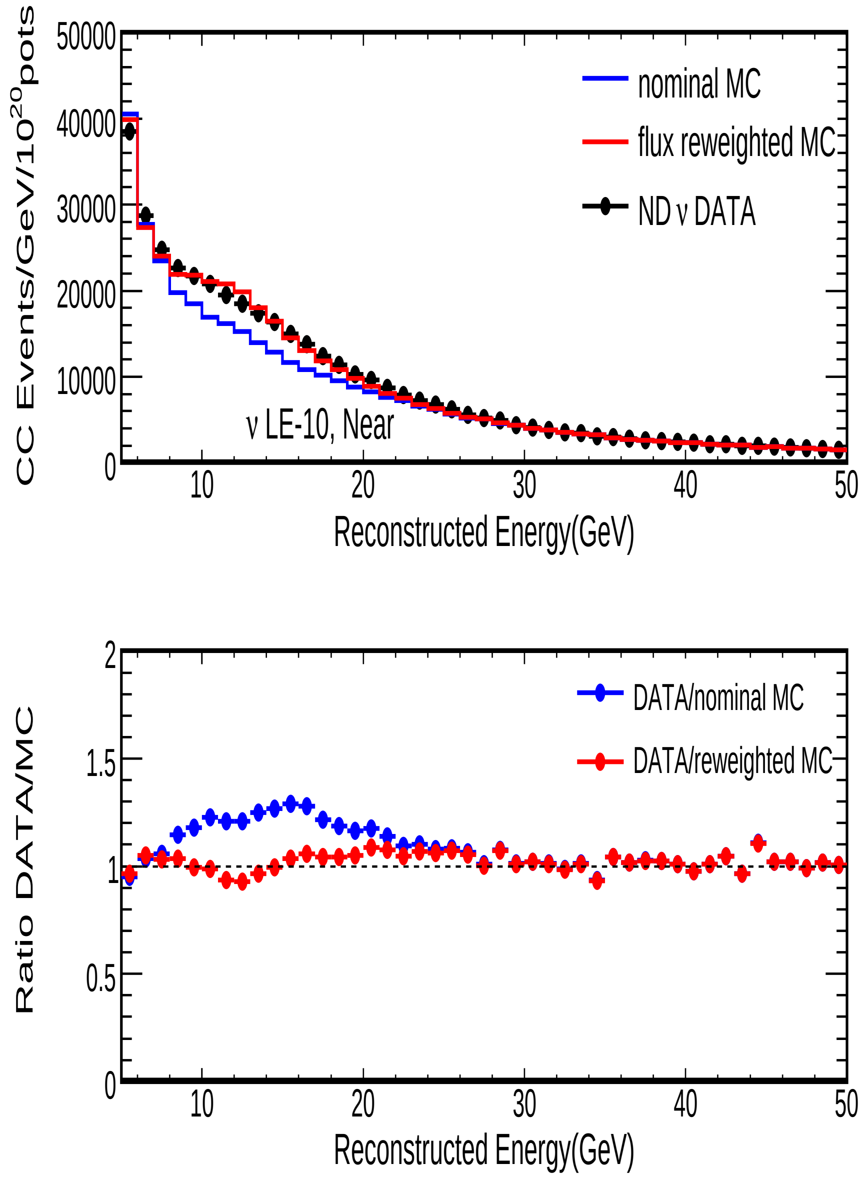

Flux Tuning in Oscillation Analysis

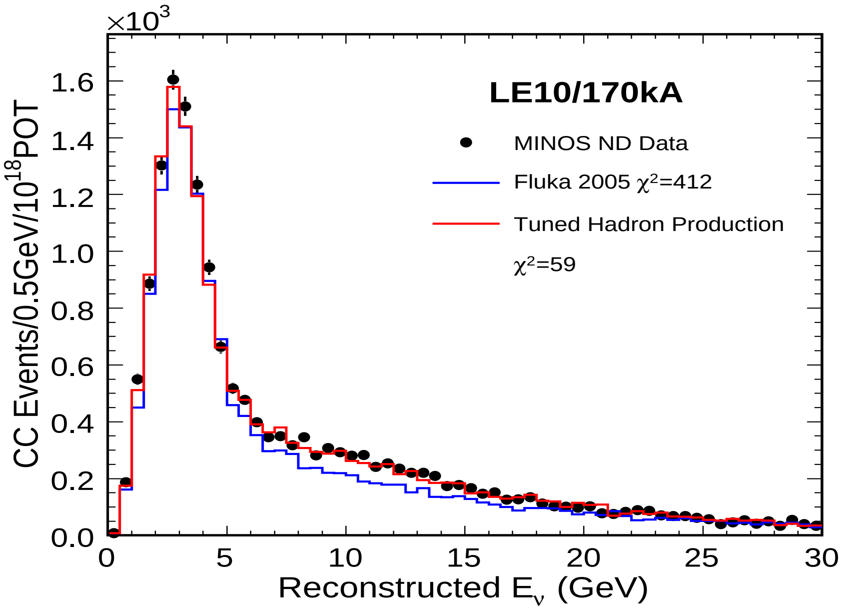

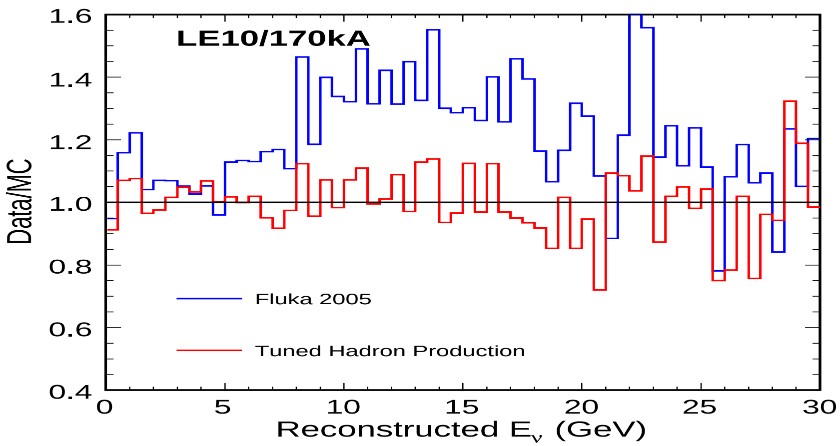

- Use reconstructed energy spectra from all beam configurations to tune production model.
  - Hadron production model, (production of pions from 120GeV protons on graphite) is adjusted by applying fitted weights as a function of (x_f, p_T) of parent pion.
- Nominal Near detector MC (blue curve) shows systematic disagreement in tail of LE beam.
- Data/MC agreement (red curve, MC after tuning) improves for LE tail.
- "Tuned" flux is also higher in the tail region, agrees with extracted low-ν flux.

Total Cross Section Energy Dependence

- $\sigma_{\rm TOT}(E) = \frac{N^{\rm corr}_{\rm xsec}}{\Phi(E)}$
  - $N^{\rm corr}_{\rm xsec}$ = cross section sample events corrected for acceptance and smearing using MC.

$$N^{\rm corr}_{\rm xsec}(\mathrm{E}) = N^{\rm raw}_{\rm xsec}(\mathrm{E}) \left(\frac{N^{\rm MCgen}(\mathrm{E})}{N^{\rm MCreco}_{\rm xsec}(\mathrm{E})} \right)$$

$N^{\rm MCgen}(\mathrm{E})$ = events generated in the fi ducial volume.

$N^{\rm MCreco}_{\rm xsec}(\mathrm{E})$ = events in the MC reconstructed sample.

- Correct to Isoscalar target, (Iron $\frac{N-Z}{A} = 0.0567$).
- Normalize in region 10-50 GeV using world average ν-Iso Fe value:

$$\left(\frac{\sigma^{\nu}}{E}\right)_{\rm world} = 0.676 \pm 0.04 \ \times 10^{-38} \frac{\rm cm^2}{\rm GeV}$$

- **Measures shape of $\frac{\sigma}{E}$ with energy.**
- **Fake-data study, comparison to NEUGEN model prediction. (3.7$\times 10^{19}$ PoT sample).**
  - **Band shows size of error on the weighted average for data points with $\mathrm{E} > 10\mathrm{GeV}$ (used for normalization).**
- **Minos full sample (7.4$\times 10^{20}$ PoT) will be $\sim$20$\times$ larger $\rightarrow$ statistical precision $\sim$4.5$\times$ better.**

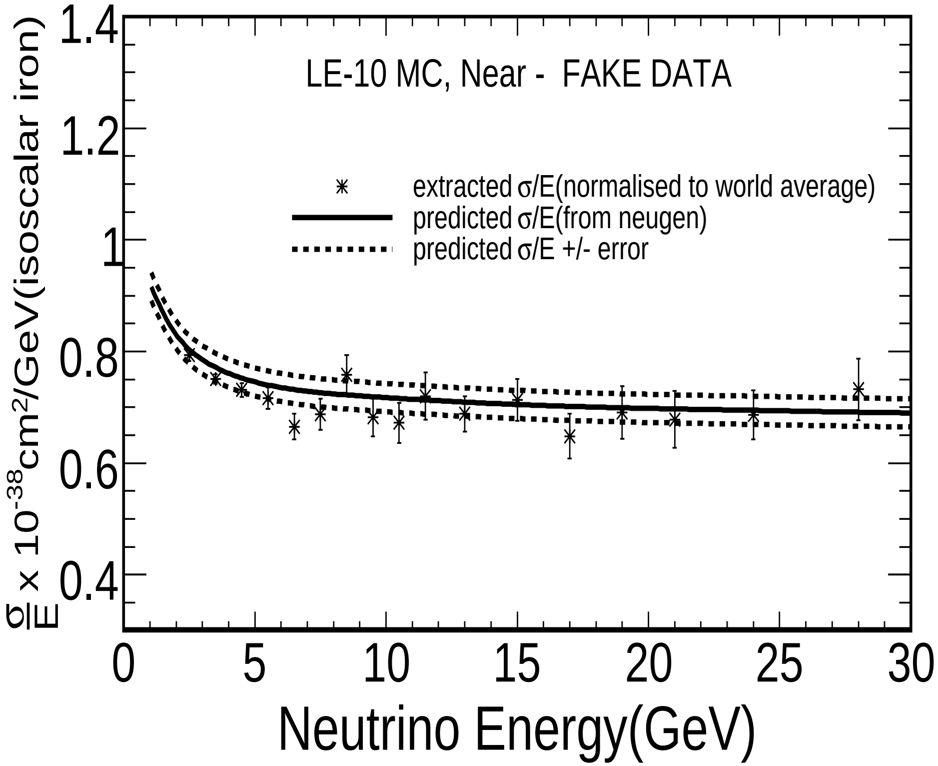

Flux and Cross Section Errors

- Low-ν Flux method valid for $E_\nu > 5$GeV
  - At lower energies systematics from model and acceptance corrections become large.
- Systematics evaluated:
  - E_μ scale $\pm$2% (Largest for Flux)
  - $E_{\rm HAD}$ scale $\pm$5.6%
  - Final state Intranuclear rescattering. (affects measured $E_{\rm HAD}$) $\rightarrow$Largest for cross section,*estimate is crude, will be reduced)*.
  - Model correction uncertainty estimate (B/A correction).
- Prognosis: Expect flux and cross section uncertainties in range 2-5% for $E_\nu > 5$GeV.

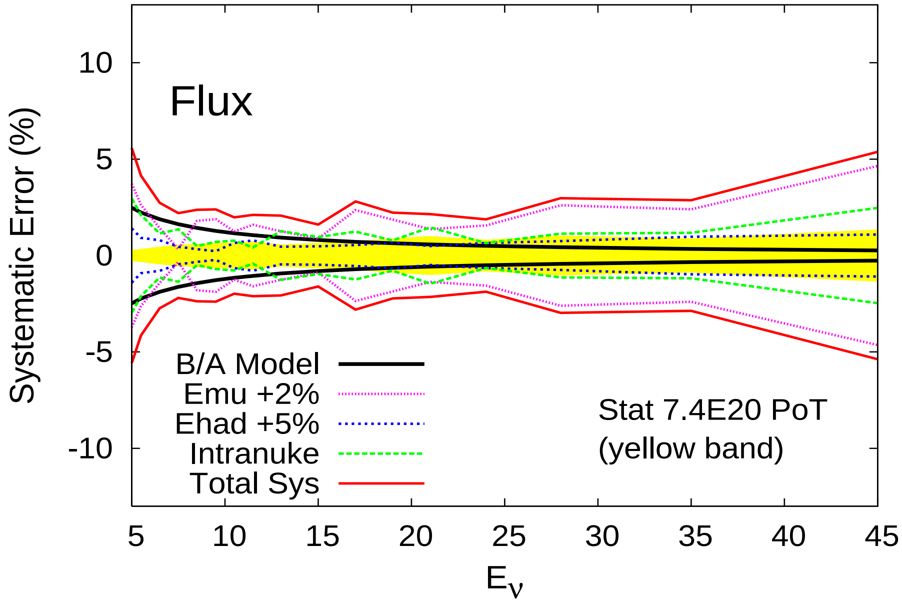

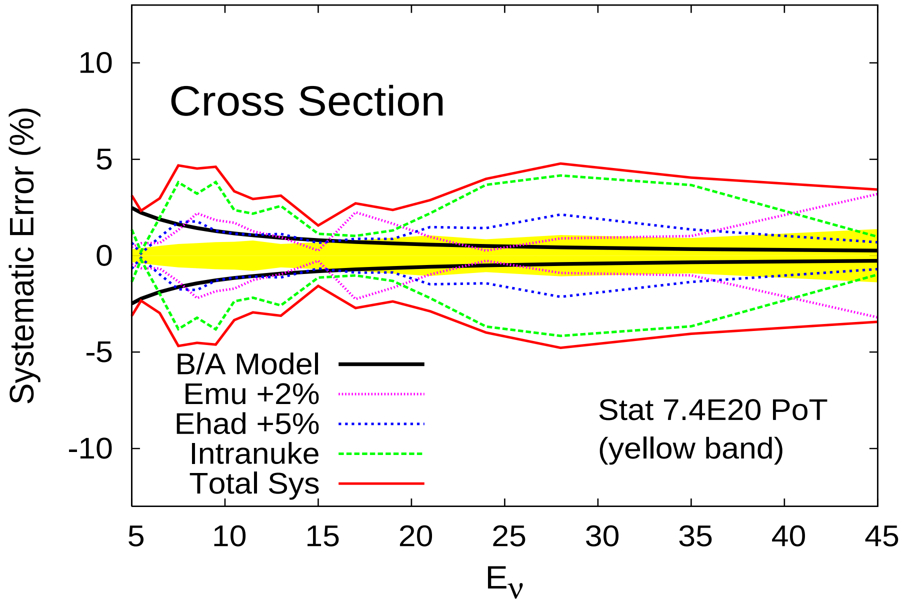

Antineutrino Sample in MINOS

- Above 5GeV $\sim$ 15% of events are from $\overline{\nu}$.
- Total expected $\overline{\nu}$-CC sample= 7.4×10^5 events for 7.4E20 PoT.
- Also studying $\overline{\nu}$ flux and cross section extraction.
  - Larger model corrections to flux.
  - Acceptance corrections (μ^+s defocussed).

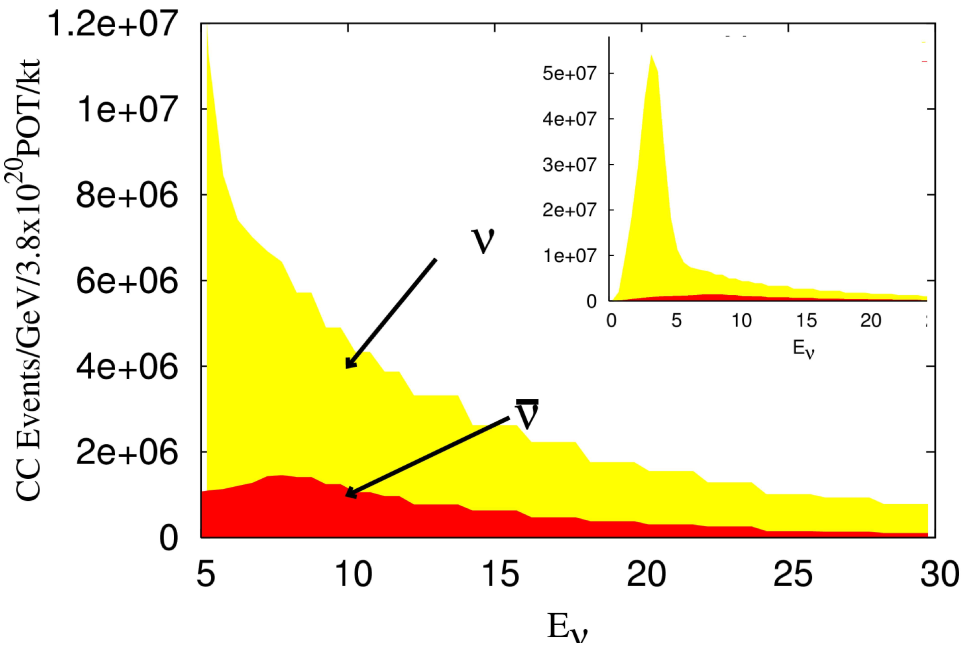

- Contamination from mis-IDed ν_μCC events is large (5-20%).
- Improvement needed to charge-sign ID to obtain high-purity sample of $\overline{\nu}$ (WIP).

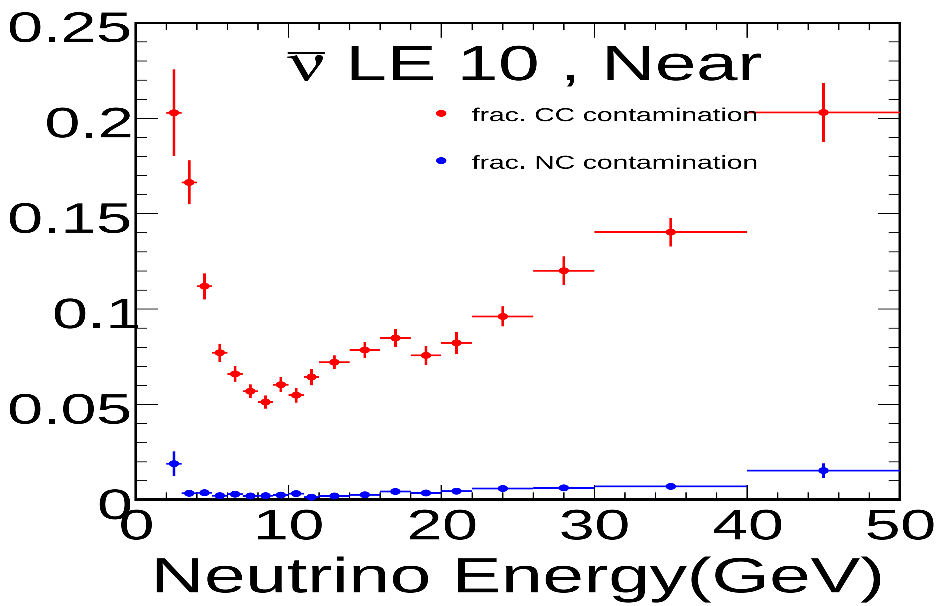

DIS Cross Section Sample

- Large data sample of DIS ($W > 2\mathrm{GeV}$) and transition region ($2 > W > 1.4\mathrm{GeV}$) events.
  - Kinematic range overlaps with SLAC and JLAB charged-lepton data sets.

ν DIS sample:

(1E20 POT LE-10)

MC: Low-ν flux rewt.

$W > 2\mathrm{GeV}$
$Q^2 > 1\mathrm{GeV}^2$
$E_\nu > 5\mathrm{GeV}$

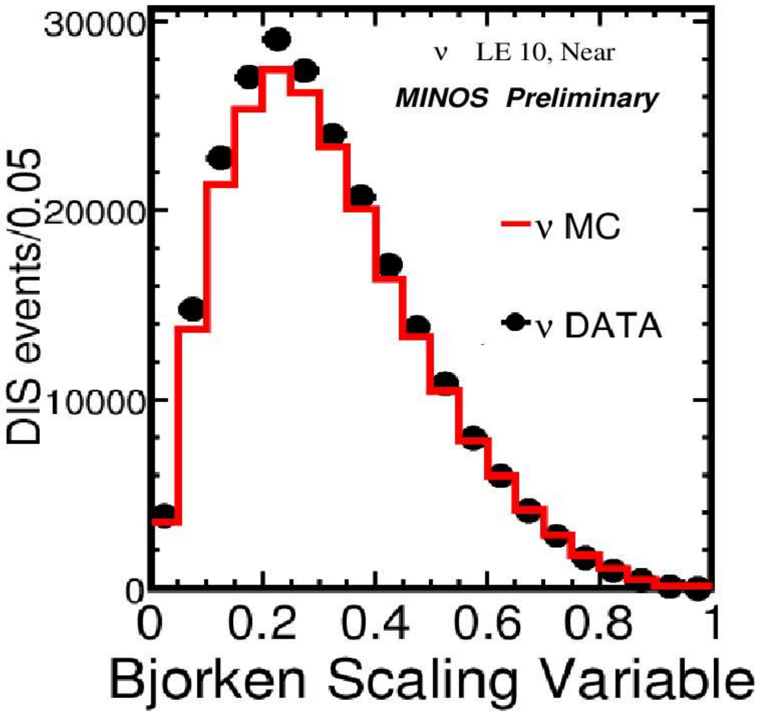

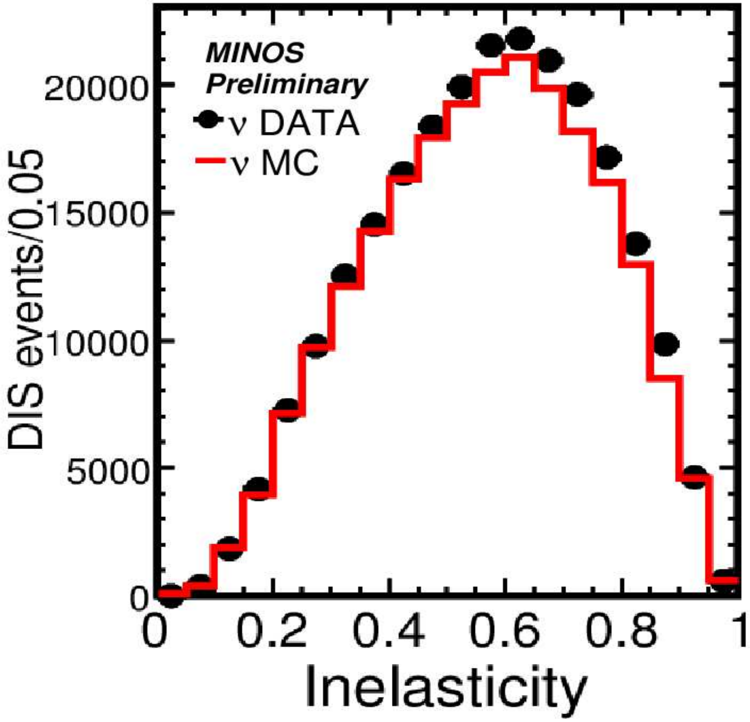

- Extract doubly differential cross section. $\frac{d^2\sigma}{dxdy}^{\nu(\bar{\nu})} = \frac{1}{\Phi(E)}\frac{d^2N}{dxdy}^{\nu(\bar{\nu})}$.
- Measure ν-Iron structure functions, $F_2(x,Q^2)$ and $xF_3(x,Q^2)$

$$\frac{d^2\sigma^{\nu(\bar{\nu})}}{dxdy} = \frac{G_F^2 M E_\nu}{\pi(1+Q^2/M_W^2)^2}\left[\left(1 - y - \frac{Mxy}{2E} + \frac{y^2}{2}\frac{1+4M^2x^2/Q^2}{1+R(x,Q^2)}\right)F_2^{\nu(\bar{\nu})} \pm y\left(1-\frac{y}{2}\right)xF_3^{\nu(\bar{\nu})}\right]$$

Structure Function Measurements

- $F_2(x, Q^2)$ from cross section sum.

$$\left[\frac{d^2\sigma^{\nu}}{dxdy} + \frac{d^2\sigma^{\overline{\nu}}}{dxdy}\right] = \frac{2MG^2E}{\pi}\left[1-y-\frac{Mxy}{2E}+\frac{1+(\frac{2Mx}{Q})^2}{1+R(x,Q^2)}(\frac{y^2}{2})\right] F_2(x,Q^2) + \left[y-\frac{y^2}{2}\right]\Delta xF_3(x,Q^2)$$

- $xF_3(x, Q^2)$ from cross section difference.

$$\left[\frac{d^2\sigma^{\nu}}{dxdy} - \frac{d^2\sigma^{\overline{\nu}}}{dxdy}\right] = \frac{2MG^2E}{\pi}\left(y-\frac{y^2}{2}\right) xF_3^{AVG}(x,Q^2)$$

  - $xF_3(x, Q^2)$ only from ν scattering.

- $F_2(x, Q^2)$ sensitivity - statistical errors only for 1.85×10^{20} PoT.
  - Systematics will be of comparable size at this level of statistical precision.

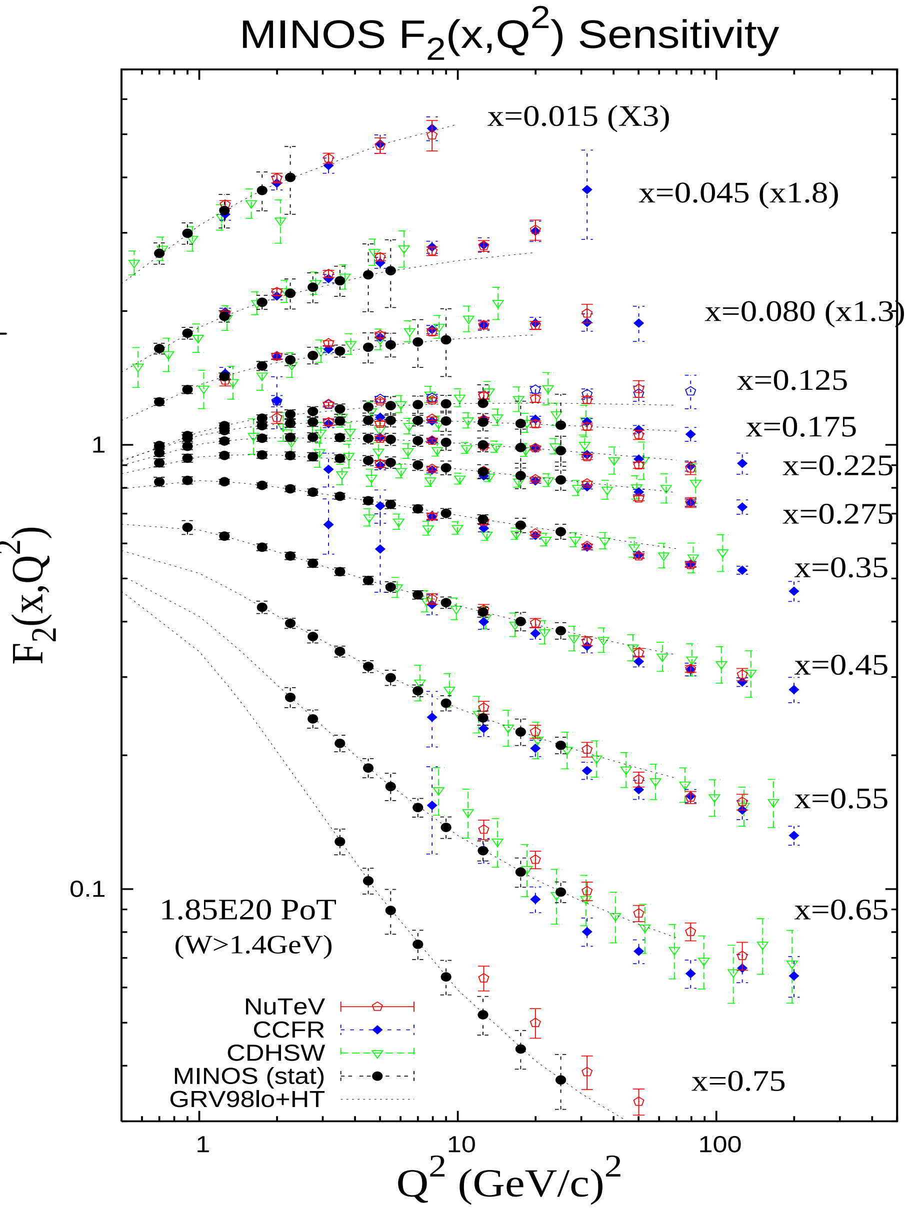

Conclusions

- First steps underway to extract CC cross sections from MINOS ND data sample.
  - Low-ν flux method applied to extract neutrino flux for $E_\nu > 5$GeV.
  - Analysis underway to extract shape of charged-current total cross section in the interesting low energy region.
  - High statistics $\overline{\nu}$ sample, studies underway to improve purity.
- Plans for inclusive ND cross section measurements:
  - Energy dependence of total cross section (ν and $\overline{\nu}$).
  - DIS differential ν and $\overline{\nu}$ cross sections.
  - Neutrino iron structure functions $\rightarrow$ New kinematic range for ν scattering.
- Also underway:
  - Quasi-elastic cross section.
  - Coherent π production
  - Dimuon production.

Backups

Hadronic Energy Resolution

Measured with test beam (CALDET) in range 1-10 GeV for pions and protons.

$\frac{\sigma}{E} = A \oplus \frac{B}{\sqrt{E}}$ quadratic

$\frac{\sigma}{E} = A + \frac{B}{\sqrt{E}}$ linear

Fits to the energy resolution for $\pi^{\pm}$ and p

	A (%)	B (%)	
π^+	4.2 ± 1.5	55.7 ± 0.5	quadratic
π^+	0.7 ± 0.4	55.1 ± 0.9	linear
π^-	0.0 ± 3.3	56.2 ± 0.3	quadratic
π^-	-0.1 ± 0.4	56.3 ± 0.9	linear
$\pi^+ + \pi^-$	2.1 ± 1.5	56.1 ± 0.3	quadratic
$\pi^+ + \pi^-$	0.3 ± 0.2	55.8 ± 0.4	linear
p	4.3 ± 1.4	56.6 ± 0.6	quadratic
p	0.7 ± 0.5	55.9 ± 1.0	linear

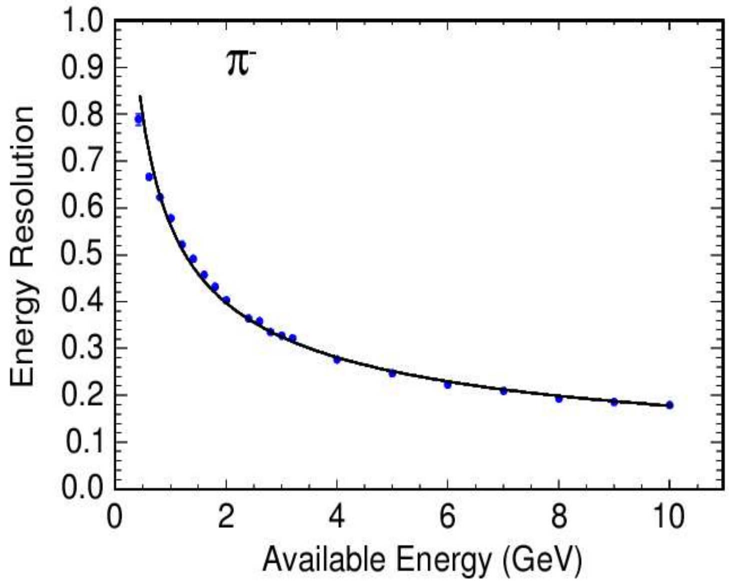

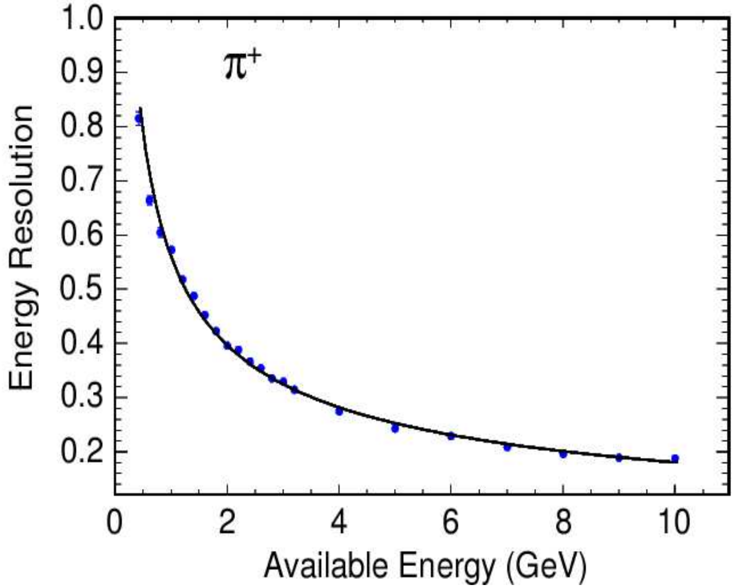

CC Selection Efficiency

Effi ciency of $E_\mu > 2$ GeV cut.

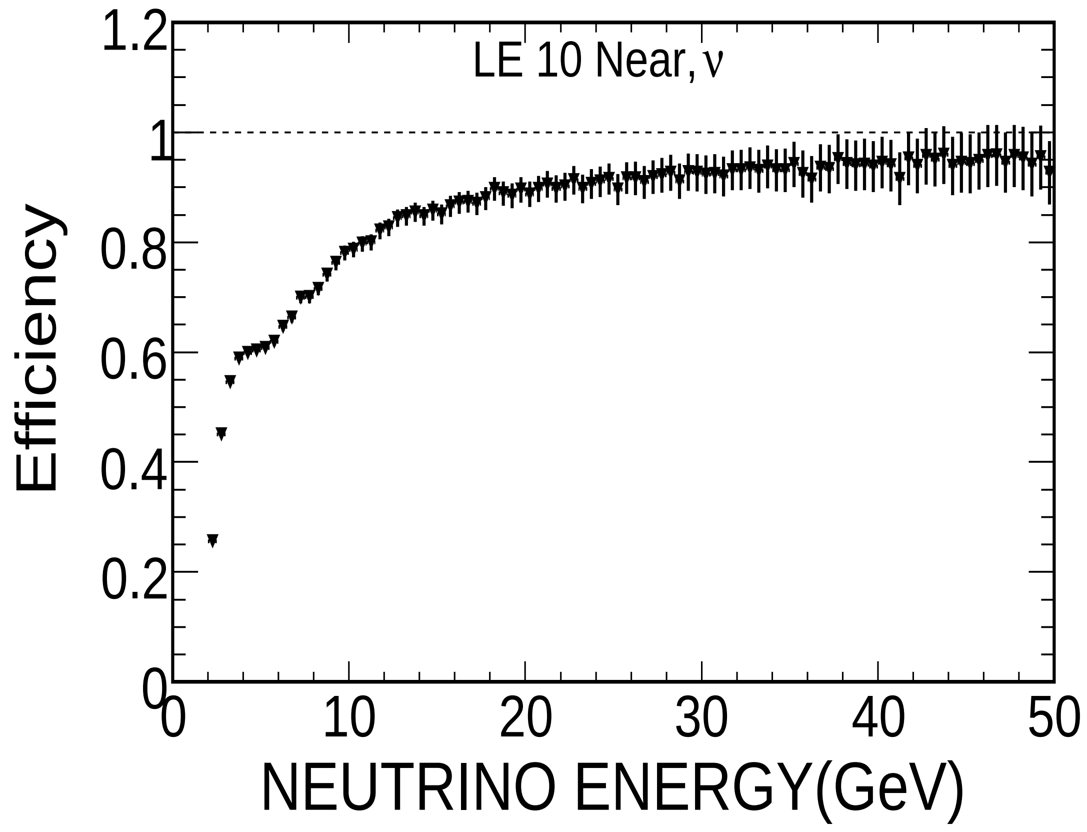

Model Corrections to Flux Extraction

Cross section model NEUGEN3 uses:

- Bodek-Yang duality model (GRV98LO pdfs tuned to data in DIS/res. overlap region.)
- QE cross section with ($M_A = 1.03$)
- No explicit contribution from resonances.
- Have also studied a NEUGEN3 version which explicitly includes resonances for $W < 1.7$ (tuned on data). resonance region.

Low-ν energy dependence of cross section components (neutrino).

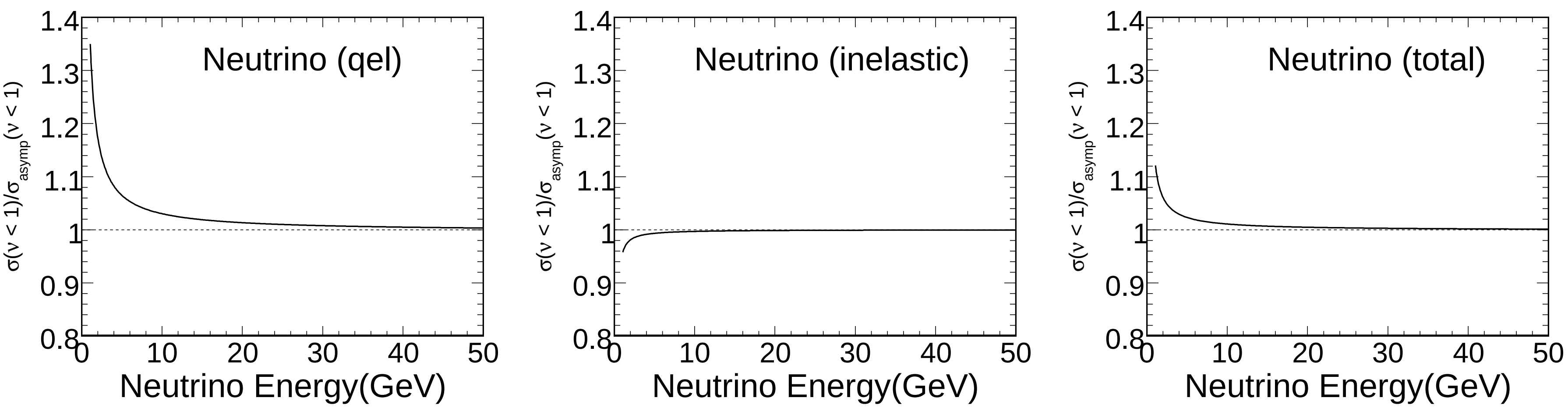

Model Corrections to Flux (Antineutrinos)

Cross section model NEUGEN3 uses:

- Bodek-Yang duality model (GRV98LO pdfs tuned to data in DIS/res. overlap region.)
- QE cross section with ($M_A = 1.03$)
- No explicit contribution from resonances.
- Have also studied a NEUGEN3 version which explicitly includes resonances for $W < 1.7$ (tuned on data).

Low-ν energy dependence of cross section components (antineutrino).

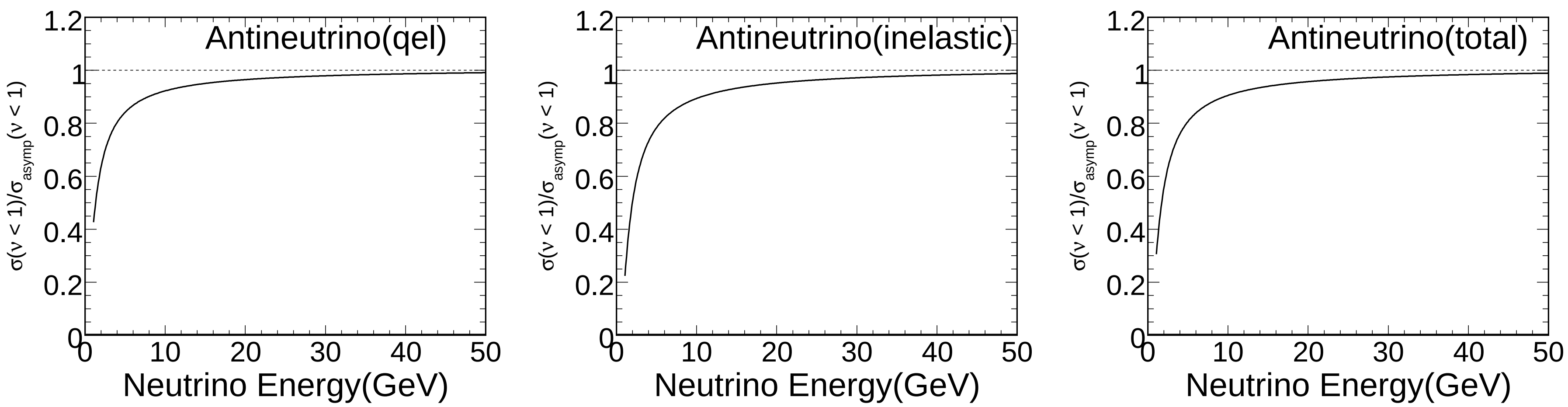

Flux Model Correction Uncertainty

Low-ν method:

$$\frac{d\sigma}{d\nu} = A\left(1 + \frac{B}{A}\frac{\nu}{E} - \frac{C}{A}\frac{\nu^2}{2E^2}\right)$$

- At low ν and high $E_\nu \rightarrow (\frac{\nu}{E})$ and $(\frac{\nu}{E})^2$ terms are small $\Rightarrow$ decreasing with energy.

$$\frac{B}{A} = -\frac{\int (F_2(x) \mp xF_3(x))\,dx}{\int F_2(x)dx}$$

- Smaller for ν than for $\overline{\nu}$
  - - for neutrinos: $-1 < \frac{B}{A} < 0$
  - + for anti-neutrinos: $-2 < \frac{B}{A} < -1$

- Theoretical value for $\frac{B}{A}$ computed from model, (problem: large uncertainty at low ν)
  - $(\frac{B}{A})^{\text{nu}}(\nu = 20) \approx -0.25$ (lower limit)
  - $(\frac{B}{A})^{\text{antinu}}(\nu = 20) \approx -1.7$ (upper limit)

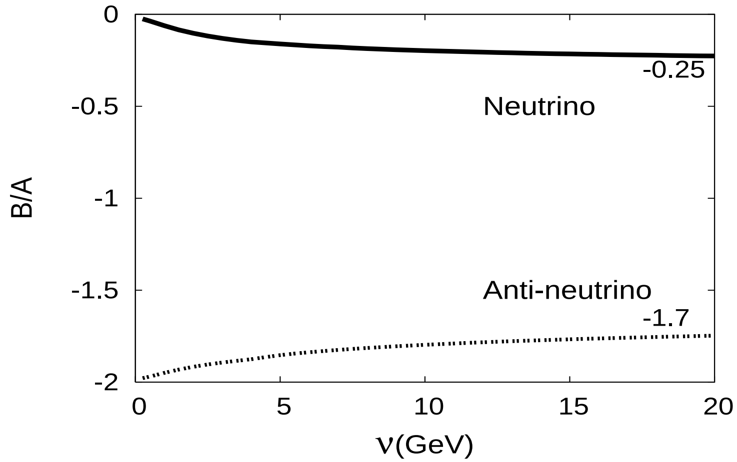

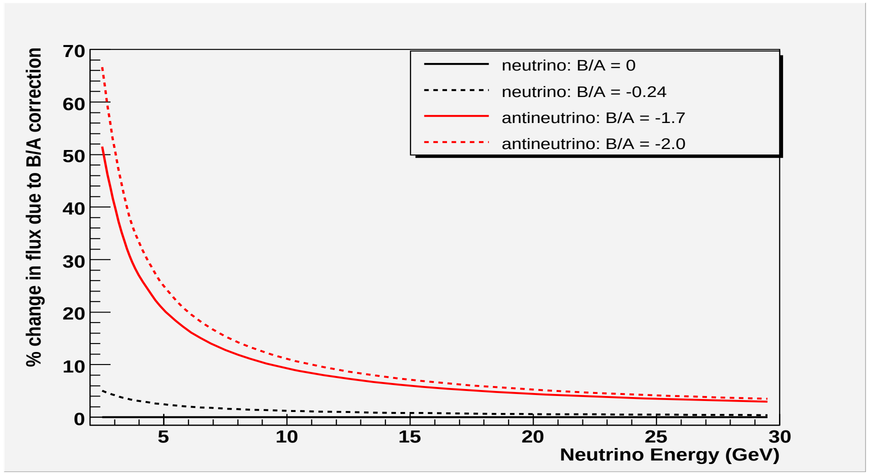

Range of DIS model uncertainty contributed by the (bounded) $\frac{B}{A}$ correction:

neutrino $0 > (\frac{B}{A})^{\nu} > -0.25$

antineutrino $-1.7 > (\frac{B}{A})^{\overline{\nu}} > -2$

Flux and Cross Section Corrections

Other physics corrections to flux and cross section

1-loop radiative corrections (Bardin), isoscalar target correction

Flux

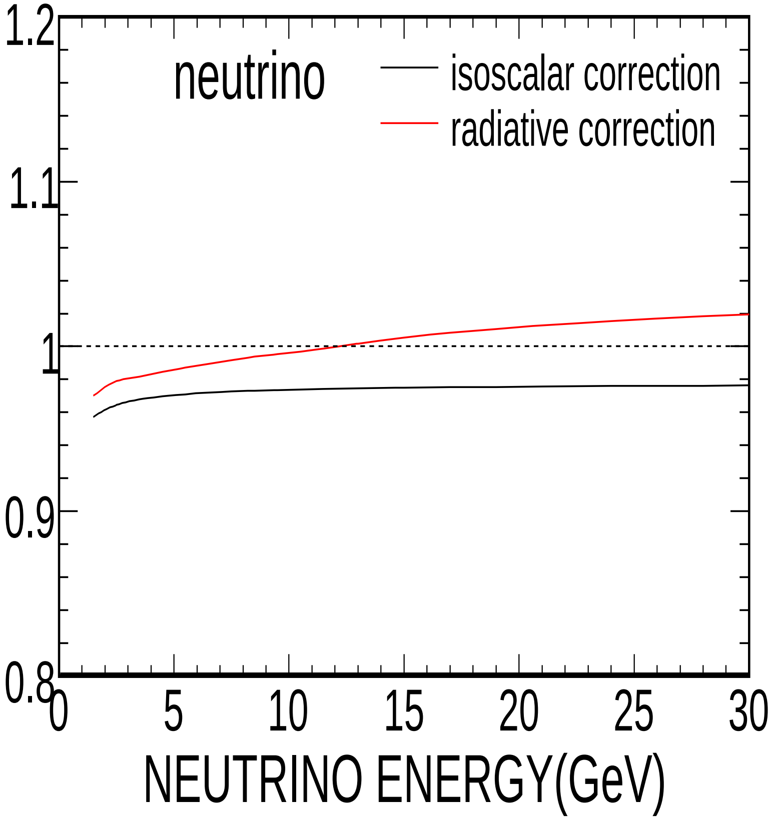

Cross Section

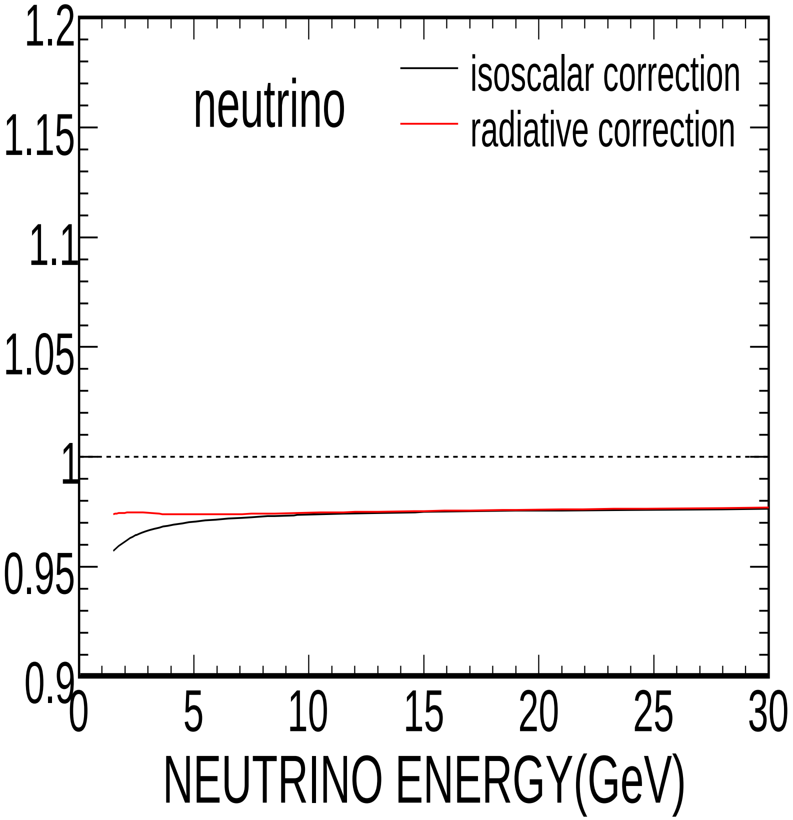

Beam Model Tuning Using ND Data

- ND data/MC disagreements are "Beam tune" dependent.
  - Detector and cross section model are common to all tunes. ▷ *implies beam modeling*
- Hadron production model (production of pions from 120GeV protons on graphite, ($f(x_f, p_t)$), is tuned to further improve data/MC agreement.
  - Fit for weights as a function of x_f, p_t for 6 beam configurations.

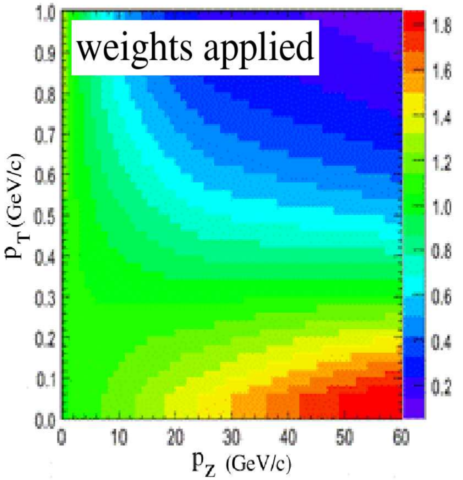

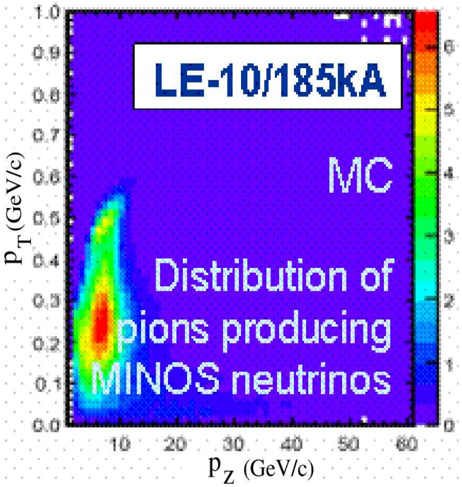

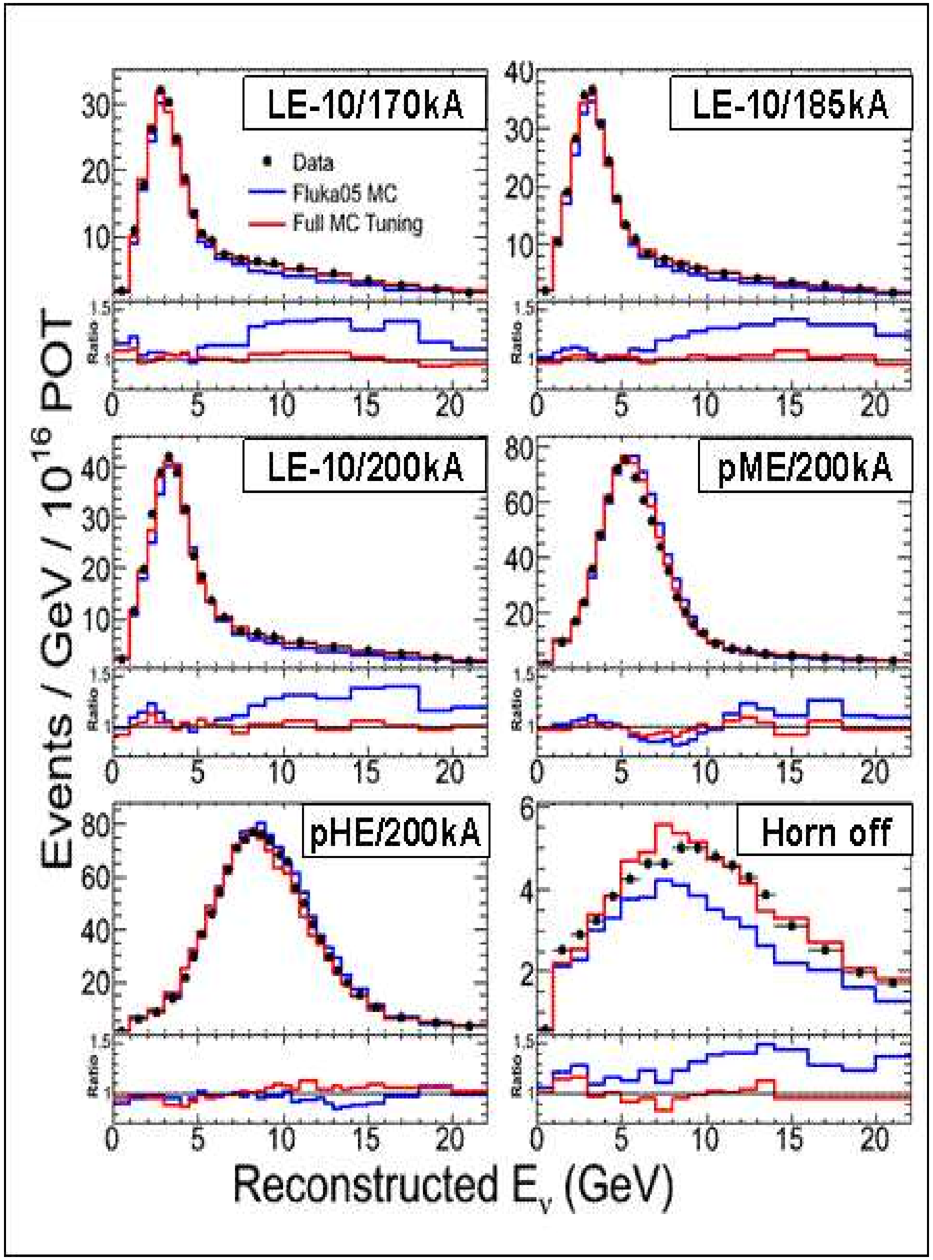

Minos Calibration System

▶LED based light injection system

- Track PMT gains.

▶Cosmic ray muons

- Remove variations along and between strips.
- Stopping muons for detector-to-detector relative energy calibration.

▶Test beam with mini-MINOS detector (CALDET)

- Measure absolute energy scales. (e,μ, π,p).

Energy Scale Uncertainties

▶ 5.7% Absolute

▶ 2% Near/Far relative

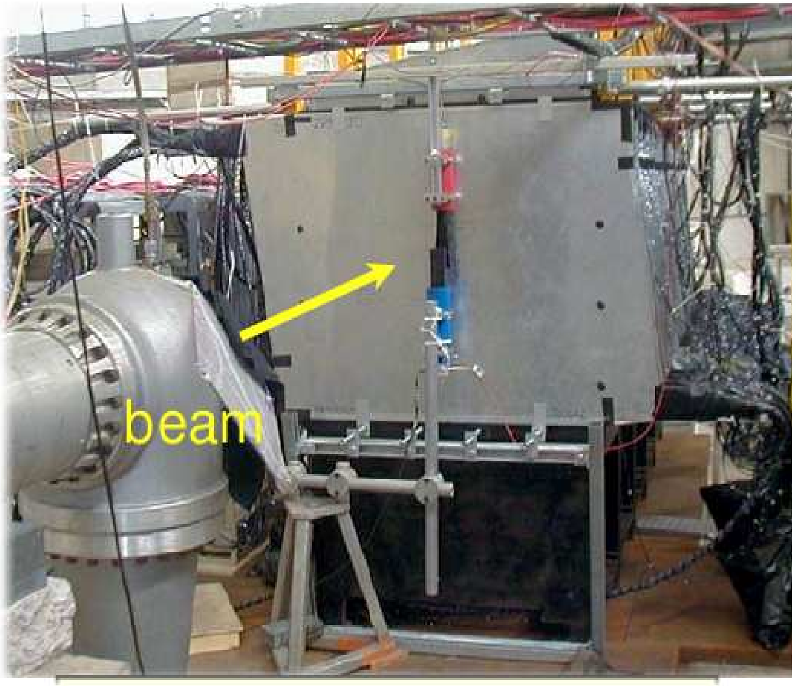

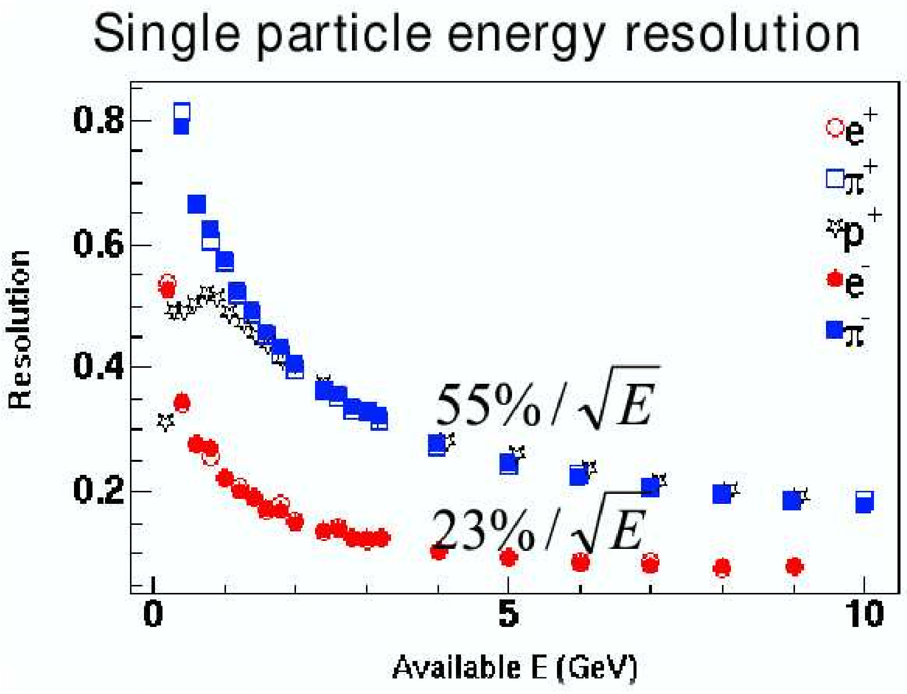

MINOS QE Selection

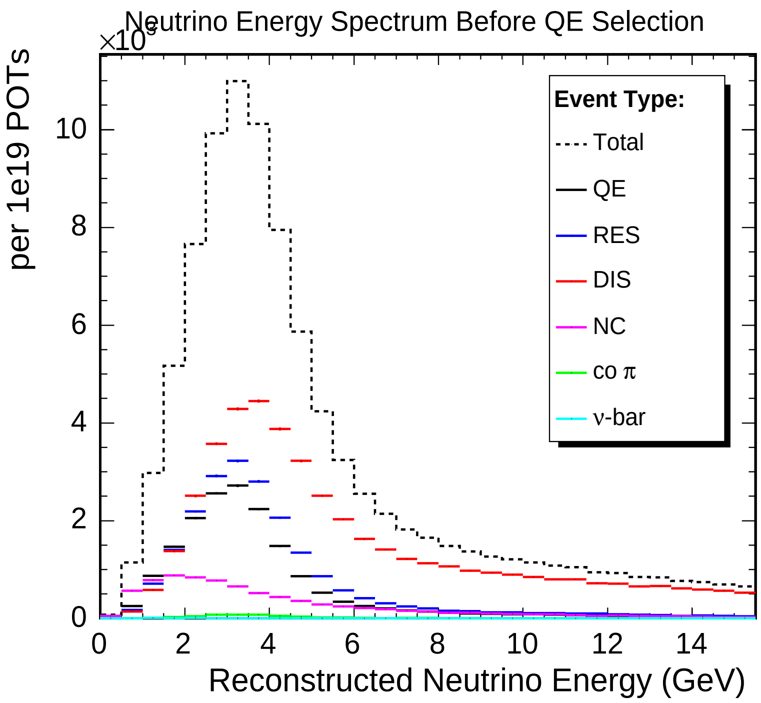

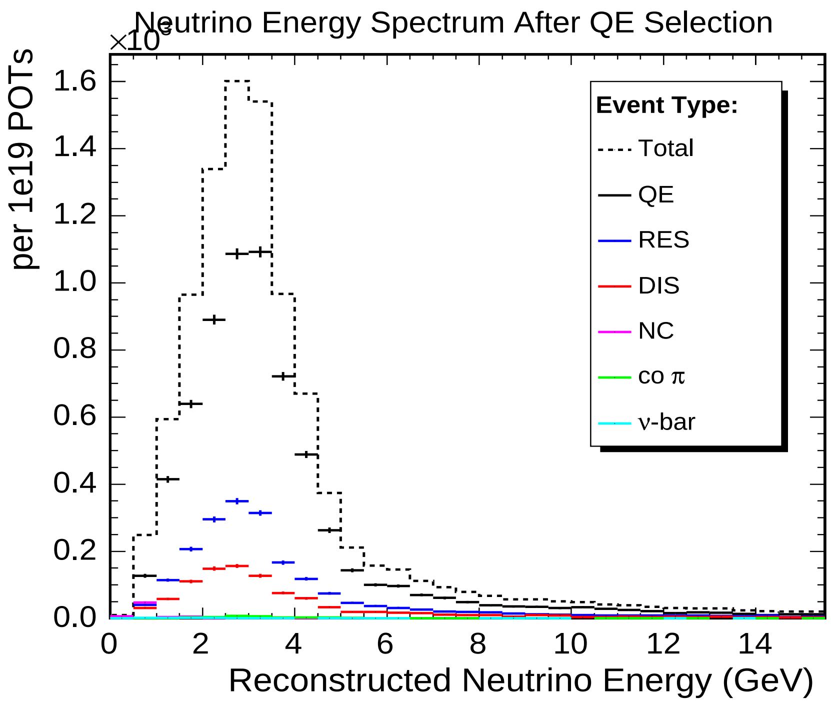

- PDF based selection based on shower topology, proton direction, reco-W.
- ∼40% efficiency, ∼70% purity.
- Modeling of low energy shower topology complicated by final state rescattering of hadronic particles.
  - Difficult to model, large uncertainty

Beam Flux Errors

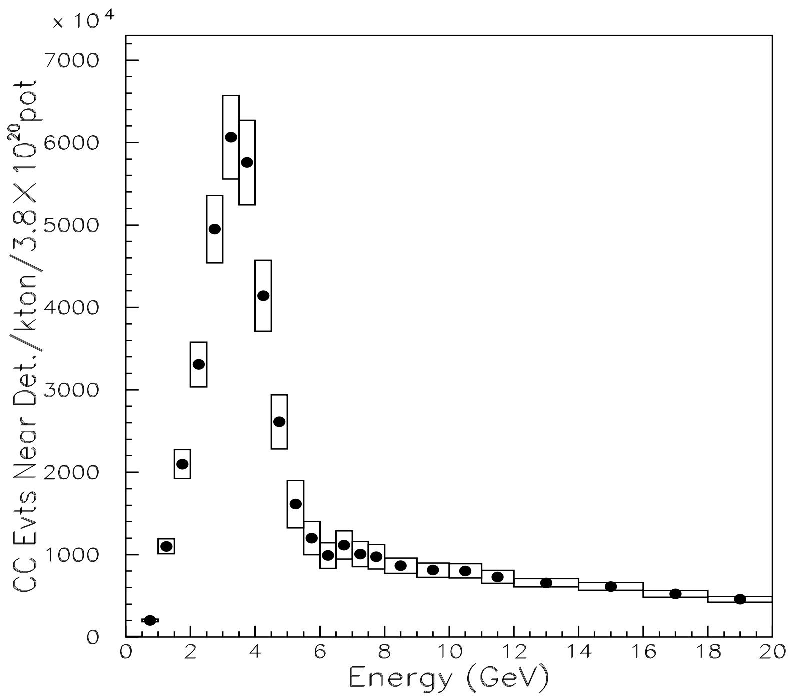

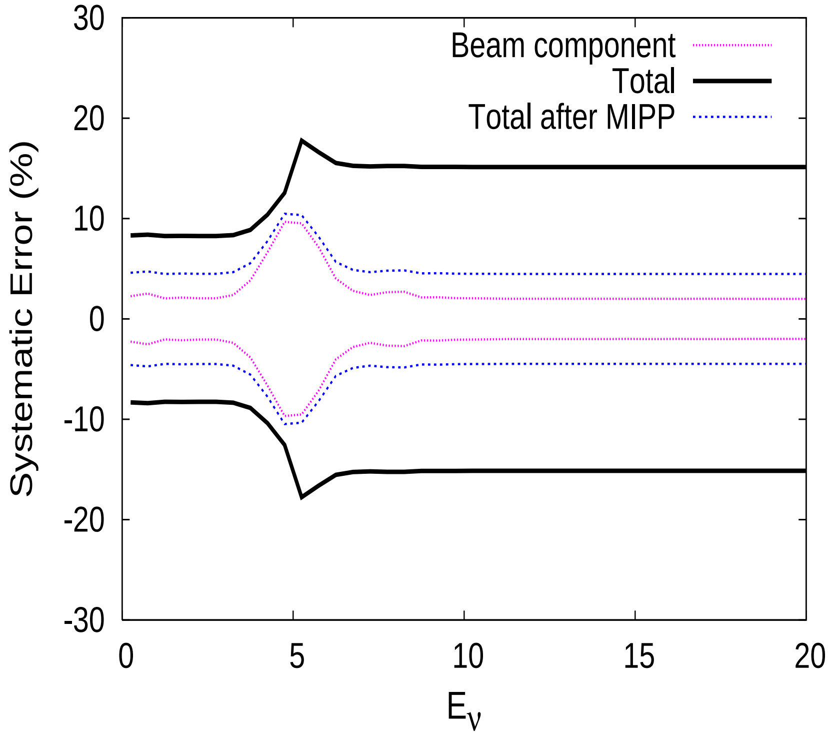

GNUMI Flux Uncertainties

- Beam component (matter most in the focusing peak region)
  1. Horn 1 offset (small)
  2. baffle scraping (small)
  3. POT (2%)
  4. Horn current offset (1%)
  5. Horn current distribution (0-8% effect)

- Production : 8-15% (15% above the beam peak).
  - Assume will be reduced after MIPP to ∼4%.

Near Detector Planes

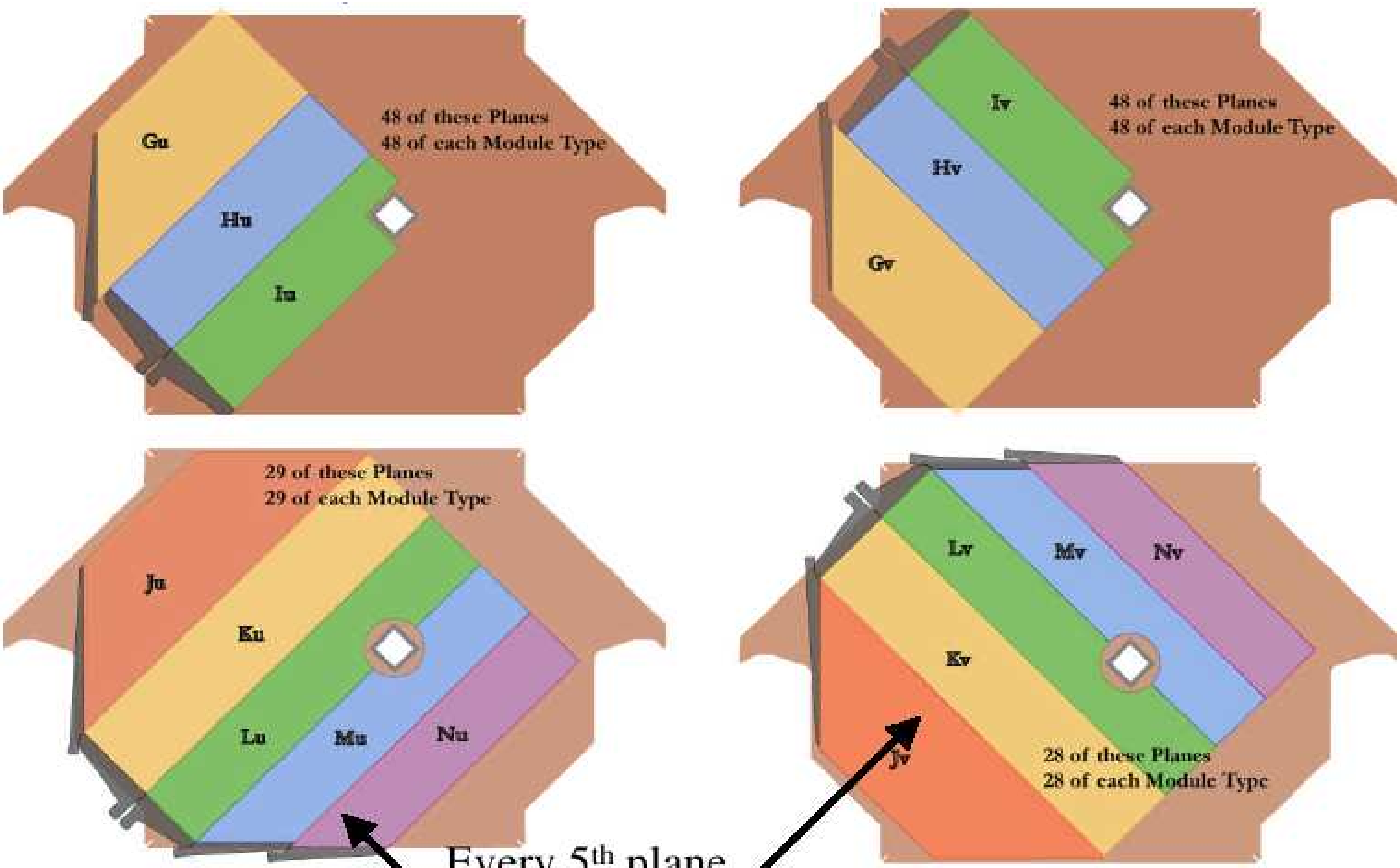

Every 5th plane throughout detector is fully instrumented

Systematics and Structure Functions

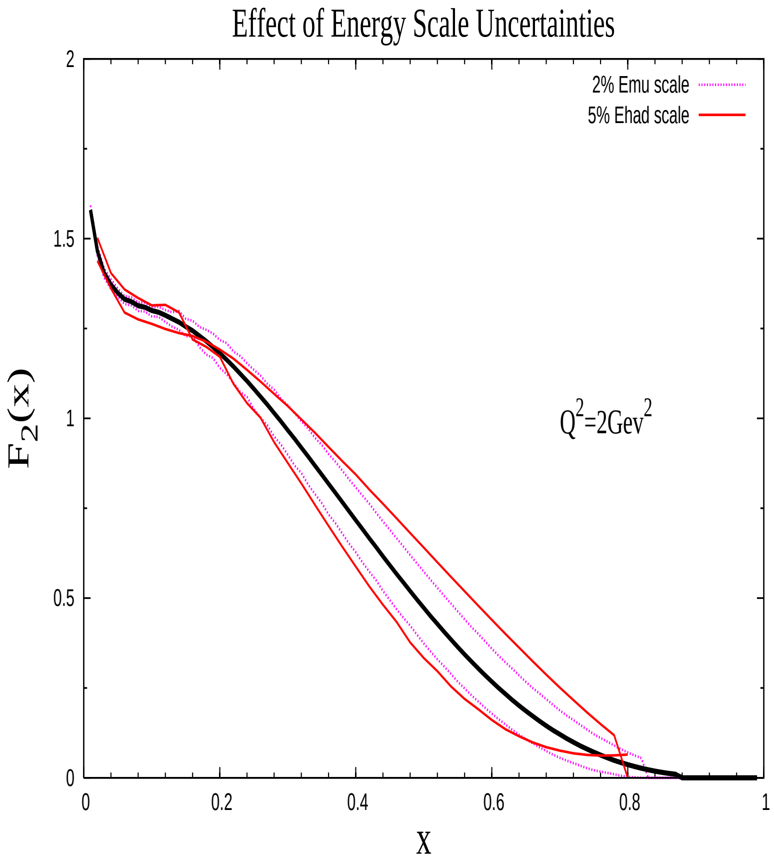

Near Detector Data

- ND sees large event rates → multiple events per 8-10μsec spill.
  - Typical intensity 2.2×10^{13} protons/spill (spill length 8-10μsec).
- Events are separated using timing and topology.
- No rate dependent reconstruction effects observed.

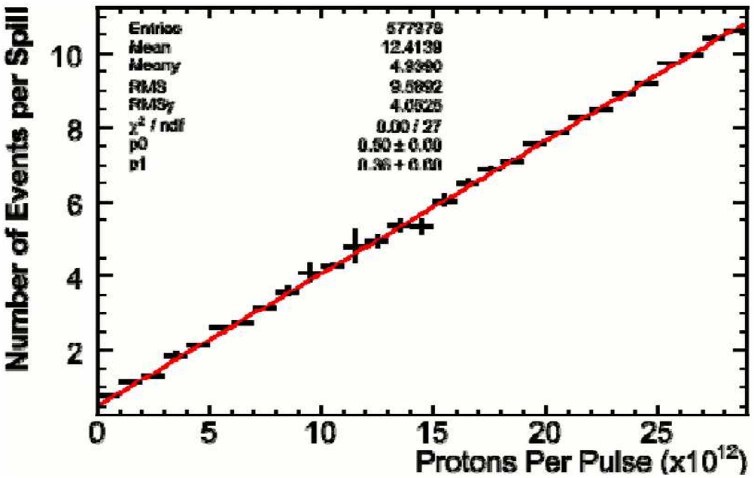

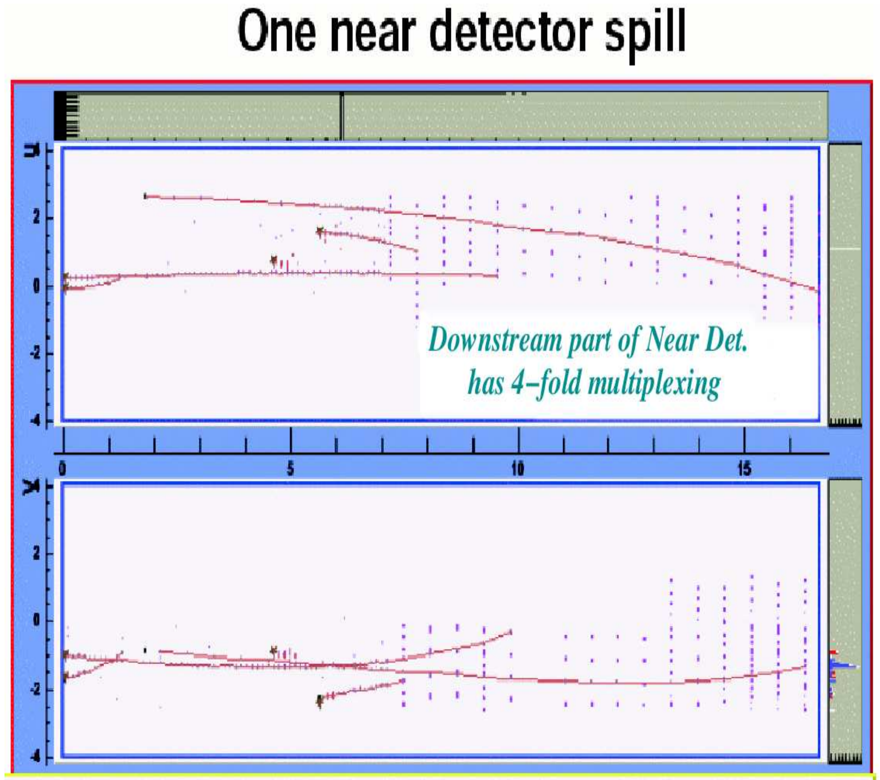

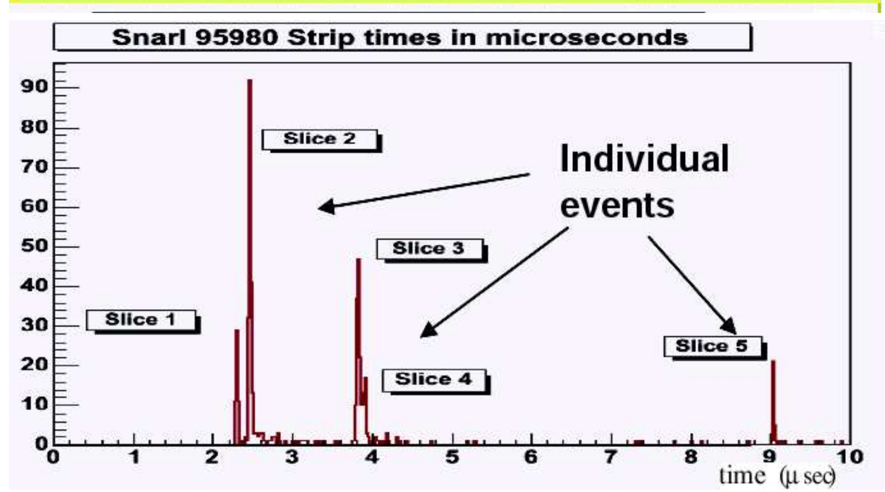

DIS Cross Section Sample

DIS events ($E_{\mathrm{HAD}} > 1\mathrm{GeV}$, $W > 2\mathrm{GeV}$, $Q^2 > 1GeV^2$, $E_\nu > 5\mathrm{GeV}$)